



REPORT NO. 1127
APRIL 1961

A THEORY FOR THE LAMINAR SUBLAYER
OF
A TURBULENT FLOW

COULLED IN

Joseph Sternberg

51005

Department of the Army Project No. 503-03-099
Ordnance Management Structure Code No. 5210.11.140
BALLISTIC RESEARCH LABORATORIES



ABERDEEN PROVING GROUND, MARYLAND

ASTIA AVAILABILITY NOTICE

Qualified requestors may obtain copies of this report from ASTIA.

BALLISTIC RESEARCH LABORATORIES

REPORT NO. 1127

APRIL 1961

A THEORY FOR THE LAMINAR SUBLAYER
OF A TURBULENT FLOW

Joseph Sternberg

Exterior Ballistics Laboratory

PROPERTY OF U.S. ARMY
STANDARD
BRL, AFG, RD. 21005

Department of the Army Project No. 503-03-009
Ordnance Management Structure Code No. 5210.11.140

ABERDEEN PROVING GROUND, MARYLAND

TABLE OF CONTENTS

	Page
ABSTRACT.	3
1. INTRODUCTION.	5
2. TAYLOR'S HYPOTHESIS IN A SHEAR FLOW	8
3. THE FLUCTUATION FIELD OUTSIDE OF THE SUBLAYER	14
4. EQUATIONS FOR THE FLUCTUATION FIELD	17
5. SIMPLIFIED THEORY	19
6. MICROSCALES	30
7. THE PRESSURE FIELD.	32
8. TURBULENCE PRODUCTION	36
9. LAMINAR-TURBULENT TRANSITION IN STRONG TURBULENCE	38
10. CONCLUDING REMARKS.	41
REFERENCES.	43

BALLISTIC RESEARCH LABORATORIES

REPORT NO. 1127

JSternberg/sec
Aberdeen Proving Ground, Md.
April 1961

*A THEORY FOR THE LAMINAR SUBLAYER
OF A TURBULENT FLOW

ABSTRACT

The so-called laminar sublayer is shown to be the region where the turbulent velocity fluctuations are directly dissipated by viscosity. A simplified linearized form of the equations of motion for the turbulent fluctuations is used to describe the turbulent field between the wall and the fully turbulent part of the flow. The mean flow in the sublayer and the turbulence field outside the sublayer are assumed to be known from the experiments. The thickness of the sublayer arises naturally in the theory and is directly analogous to the inner viscous region for the fluctuations in a laminar flow. It is shown that the large scale fluctuations containing most of the turbulent energy are convected downstream with a velocity characteristic of the middle of the boundary layer. Thus Taylor's hypothesis does not apply to these large scale fluctuations near the wall. The convective velocity found in the measurements of pressure fluctuations at the boundaries of turbulent flows is in accord with the theory. Calculations are given for the energy spectra and u' fluctuation level in the sublayer and other aspects of the fluctuation field are discussed. It is shown that the production of turbulent energy is a

*A preliminary account of this work was presented to the Annual Meeting of the Fluid Dynamics Division, American Physical Society, in November 1959 at Ann Arbor, Michigan.

maximum where the laminar shearing stress is equal to the turbulent shearing stress. The linear pressure fluctuation field at the edge of the sublayer is calculated and found to be much larger than the non-linear field. Examining the effect of strong free stream turbulence on laminar boundary layer transition, it appears that the physical model underlying Taylor's parameter is incorrect.

1. INTRODUCTION

The laminar sublayer has been a subject of controversy and investigation for more than 20 years. The reason for this interest is that the nature of the flow close to the wall has an important influence on the heat, mass, and momentum transfer from the boundary. Furthermore, experiments have shown that the flow of energy from the mean flow to the turbulent motion is a maximum inside the sublayer. This fact suggests that an understanding of the structure of turbulence in a shear flow may depend on an understanding of the flow near the wall.

The original idea, Taylor (1916), was that in a turbulent flow there ought to be a thin fluid layer next to the surface free of turbulent motion, a true laminar layer. Studies of the stability of Couette flow (the flow between a fixed wall and a moving wall) had shown that there was a critical Reynolds number $Re \approx 300$ below which all eddies would die out. The critical Reynolds number Uh/ν was formed using the velocity U of the moving wall and the separation distance h where ν is the kinematic viscosity. It was postulated that the flow next to the wall was equivalent to a Couette flow. The laminar sublayer thickness δ_s could then be estimated by substituting δ_s for the separation distance in the stability analysis.

In 1932, Fage and Townend studied the fluctuation field close to the surface using an ultramicroscope for following minute particles in water. They found no evidence of an eddy-free region near the wall. An interesting discussion of this work is given by Taylor (1932) who examined the possible connection between special types of disturbances where the velocity distributions were known and the turbulent fluctuation field found by Fage and Townend. These experimental results were confirmed by later hot-wire measurements in air by Laufer (1950, 1953) and Klebanoff (1954). Instead of being eddy free, the turbulence level, as given by the ratio of u' the root-mean-square value of the velocity fluctuation in the flow direction to the local mean velocity U_ℓ , reached a maximum value

of approximately .4 close to the wall. Also the turbulent shear stress, as deduced from the mean flow measurements, did not vanish in a thin region next to the wall but instead varied continuously from zero at the wall to the level of the wall shear. Thus it has been clear for some time that a theory of the "laminar" sublayer must account for the fact that the flow is turbulent all the way to the wall.

There is now a relative wealth of experimental information on the fluctuation field close to the wall of a turbulent flow. What is needed is a theoretical structure that will provide a rational foundation for the understanding and interpretation of the experimental observations. Several recent attempts have been made to develop phenomenological models for the flow in the sublayer. On the basis of some observations using dye in water, Einstein and Li (1956) were led to postulate the periodic growth and decay of a true laminar region near the wall. An equivalent model has been proposed by Hanratty (1956). However, in all these cases, agreement with the measurements of the mean and fluctuation field is sensitive to the choice of critical parameters as well as to arbitrary and sometimes inconsistent assumptions concerning the physical processes. The purpose of this paper is to make a start toward the development of a theory for the sublayer which follows from the Navier-Stokes equations without the need for phenomenological assumptions or tinkering with adjustable parameters.

We have already suggested that the sublayer is only a special part of the general turbulent fluctuation field in a bounded shear flow. The aim of the theory will be to describe as far as possible the direct influence of the wall on the fluctuation field. The turbulent field outside of this region of direct influence is assumed to be known on the basis of the experimental measurements. This knowledge is essential in the development of the sublayer analysis. Fortunately we need not be concerned with shear flow turbulence in all its complexity, since only certain, fairly simple, aspects of such flows are significant for this problem. However, some of the simple features have been obscured by

the accepted methods for presenting the experimental results. It is customary to determine the space scales or wave numbers for the turbulent measurements by using Taylor's hypothesis (Taylor 1938) to justify the necessary space-time transformation. Our first step will be to show that this hypothesis, which was introduced to represent the turbulence behind a grid in a wind tunnel, is not valid in a shear flow especially near a wall. This analysis will provide a basis for re-interpreting the experimental measurements and will make possible some important simplifications in the subsequent development of the theory.

2. TAYLOR'S HYPOTHESIS IN A SHEAR FLOW

Taylor's hypothesis, which has been amply verified for a uniform low turbulence flow involves two assumptions:

- a) The turbulence pattern is convected past the measuring point with the local mean speed.
- b) The turbulent fluctuating velocities are small enough compared to the mean motion to insure little change in the shape of an eddy as it is carried past a fixed point.

The use of this hypothesis in a shear flow has previously been questioned by Lin (1953). Essentially, Lin investigated the conditions for negligible eddy distortion, and showed that there is "no general justification of extending Taylor's hypothesis to the case of shear flow". He found that unless an eddy component had a scale much less than the boundary layer thickness, it would suffer significant distortion due to the mean flow shearing motion while being carried past the measuring point by the mean flow. However, Lin's analysis did not lead to an alternate procedure for determining the turbulence scales.

We will show that, in general, assumption (a) cannot be valid in a turbulent shear flow. The departure from this assumption in a boundary layer is especially significant near the wall.

Consider a turbulent boundary layer on a flat plate. At any instant t , the turbulent fluctuation field in a boundary layer can be represented by a distribution of disturbance vorticity components ξ , η , and ζ throughout the boundary layer. At the wall the vertical perturbation velocity v must vanish. This boundary condition can be satisfied by adding an image vorticity distribution on the opposite side of the wall. Now, associated with the vorticity at a point P' in the boundary layer, there is an induced velocity at the point P . The total velocity perturbation at point P at any instant can then be found by integrating over the boundary layer and image system perturbation vorticity fields. The extent of the region over which the integration must be carried out

depends on the scale of turbulence. If only small scale motions are present then the region of integration can be confined to the vicinity of P. There should not be any significant correlation between velocities at point P and random small scale vorticity at distances from P many times the scale of the disturbances. If large scale motions are present then the integration must extend at least over the distances where these large scale motions are significantly correlated.

A typical one dimensional energy spectrum for the velocity perturbation u in the flow direction at $y/\delta = .58$ near the center of a boundary layer is shown in Fig. 1, where y is the distance from the wall and δ is the boundary layer thickness. If we can assume for the moment that this disturbance field is being carried along by the mean flow in accordance with Taylor's hypothesis, then the frequency can be converted into a measure of the space scale L by the relation $L = U_\ell / f$ where U_ℓ is the velocity of the local mean flow (we will show that this is justified in the central region of the boundary layer).

Figure 1 also shows the contribution to the total energy $\overline{u^2}$ as a function of the scale of the motion. It is evident that fully half of the energy is contributed by turbulence whose scale is more than twice the boundary layer thickness, as first noted by Townsend (1951). Thus the velocity perturbation at a point P does not depend significantly on the vorticity in the immediate vicinity of P, but rather on the vorticity over an extensive region of the boundary layer.

Since the vorticity travels with the fluid particles, the apparent velocity with which a disturbance sweeps past the measuring point P may therefore be substantially different from the local mean velocity at P. For the large scale motions, this disturbance velocity will correspond to the mean velocity near the middle of the boundary layer. Therefore for points P close to the wall, where the mean velocity is low, we would expect the disturbance velocity to be greater than the local mean velocity; for points P near the outer edge of the boundary layer, the disturbance velocity should be less than the local mean velocity.

The space-time correlation data of Favre, Gaviglio, and Dumas (1957, 1958) provide a basis for determining whether these deductions are correct. If $F(f)$ represents the percent of turbulent energy associated with the frequency f , and Taylor's hypothesis is satisfied, then the auto-correlation coefficient R_x of the u' fluctuation at the points P and $(P+x)$, can be written as

$$R_x = \int_0^{\infty} F(f) \cos \left[\frac{2\pi x}{U_\ell} f \right] df$$

where

$$R_x = \frac{\overline{u(P) \cdot u(P+x)}}{\overline{u^2(P)}}$$

The longitudinal correlation coefficient calculated in this way should then agree with the longitudinal correlation coefficient directly measured with two hot wires.

This autocorrelation coefficient has been calculated using the energy spectrum measured at one of Favre's test points and is shown in Figure 2. The integration is only carried out to $f_{\max} = 1000$ c.p.s., but this includes 98% of the energy. In Figure 2, two additional correlation curves are shown for which the integration was terminated at smaller values of the frequency therefore eliminating the contribution of the small eddies. A frequency of 400 c.p.s. corresponds to a longitudinal scale of about 2.4 centimeters which compares with a boundary thickness of 3.4 centimeters. It is evident that the correlation coefficient at large distances is not significantly affected by the small eddies. We shall confine our attention to the portion of the correlation curve determined by the large scale eddies so that R_x will be less than .4.

If the velocity of the disturbance U_w , associated with these large scale eddies differs from the local mean velocity U_ℓ , U_w rather than U_ℓ must be used in the formula for computing the correlation coefficient from the energy spectrum at a fixed point. Thus, at a fixed value of

R_x the computed correlation curve should be shifted horizontally where the new horizontal coordinate $x' = x \cdot U_w/U_\ell$. Only the portion of the curve dominated by the large eddies should be shifted in this way, since as the eddy size is reduced, the disturbance velocity approaches the local mean velocity.

One of the figures from Favre's paper (1958) is reproduced in Figure 3. Auto-correlation curves using Taylor's hypothesis and longitudinal space correlations measured with two hot wires are shown for four positions across a boundary layer. While there is the usual experimental scatter, there is a systematic difference between the two sets of curves below $R_x \approx .4$ depending on the location of the measuring point in the boundary layer. Close to the wall the measured longitudinal correlation curves are to the right of the calculated auto-correlation curves. Near the outer edge of the boundary layer, the measured longitudinal correlation curve is displaced in the opposite direction. At $y/\delta = .24$ the difference between the two curves is lost in the scatter of the data.

As far as they go, these measurements are consistent with the picture in which the large scale disturbances which contain most of the energy move down stream at a mean velocity characteristic of the central region of the boundary layer fluid. At $y/\delta = .24$ in Favre's boundary layer, the velocity U_ℓ is approximately equal to $.78$ of the free stream velocity U_1 . The horizontal shift in the correlation curve that would be expected at $y/\delta = .03$ if the disturbance velocity were equal to $.78 U_1$ is also shown in Figure 2. This shift is approximately the same magnitude as the shift found in Figure 3. A similar divergence of the calculated auto-correlation and measured longitudinal correlation coefficients at large scales has been observed by Klebanoff and led him to remark that "this divergence gives rise to the interesting speculation that the large scale motions have their own characteristic velocity different from the mean speed".

We conclude, on the basis of this analysis, that in a boundary layer, or in fact, in any shear flow, the disturbance velocity at a measuring point P is in general different from the local mean velocity. Therefore, the customary conversion of experimental spectral measurements into wave numbers is invalid in a boundary layer anywhere near the wall except for the small scale structure of the turbulence.

In the following sections of this paper, many of the numerical results will be based on the experimental measurements of Klebanoff. The limited auto-correlation and longitudinal correlation measurements he made do not extend to large enough scales to establish a value for the disturbance velocity of the large eddies with any precision. Accordingly, we shall use the general information obtained from Favre's data and somewhat arbitrarily set $U_w = .8U_1$ for the large eddies. This is the value of the mean velocity at $y/\delta = .27$. We will also need to establish an approximate upper limit to the frequency range to which this disturbance velocity applies. Klebanoff's auto and longitudinal correlation measurements indicate that for $R_x < .5$, the expected shift of the longitudinal correlation curve with respect to the auto-correlation curve will have occurred. Calculations for R_x as a function of frequency at different separations are shown in Figure 4 for $y/\delta = .05$. If we consider the curve for $x/U_\ell = 1.8$, it is evident that the frequencies > 300 make a minor contribution to the correlation coefficient. That is, the frequencies between 300 and 1000 only produce a moderate oscillation about the final value of $R_x = .43$. A frequency of 300 c.p.s. corresponds to an eddy scale of $L = U_w/f = 4$ cm or approximately $(1/2)\delta$. (Frequencies between $0 < f \leq 300$ c.p.s. account for about 80% of the fluctuation energy). We will therefore limit the specification $U_w = .8U_1$ to frequencies from $0 \rightarrow 300$ c.p.s. For high frequencies, or small scale motions, the disturbances move downstream with the local mean velocity. A very crude guess for the dependence of disturbance velocity on frequency at $y/\delta = .05$ will be given in the section on the microscales. But Klebanoff's experimental data do not provide any clear basis for guessing at this dependence in the sublayer. As will be

mentioned in the section on the pressure field, it may be possible to establish the variation of disturbance velocity with frequency for the higher frequencies from the measurements of wall pressure fluctuations. But at the present this information is not available and this lack of knowledge will necessarily limit certain possible applications of the present theory.

3. THE FLUCTUATION FIELD OUTSIDE OF THE SUBLAYER

When the experimental measurements themselves are examined, they reveal a rather striking similarity of the energy spectra at different points in the fully turbulent part of the flow. The normalized energy spectra across a boundary layer as measured by Klebanoff are shown in Figure 5. Over the inner half of the boundary layer, in the region free of intermittency, the spectra for the energy containing eddies appear to agree within the experimental error. Differences in the high frequency end of the spectra would be revealed by using a log scale rather than a linear scale, but these portions of the spectra provide a negligible contribution to the total fluctuation energy. The same results are found for pipe or channel flow spectral data. This similarity of the energy containing portion of the frequency spectra is just what would be expected from the previous analysis since the disturbance velocity for the large scale eddies should not vary significantly across the shear flow. At each point across the boundary layer, the hot-wire probe responds to disturbances associated with the same large scale eddy pattern and so the spectral distribution should be similar.

On the other hand, the fluctuation energy varies from point to point. Figure 6 shows the variation of the root-mean-square fluctuation velocities u' , v' , and w' across the boundary layer. It can be seen that the u' fluctuation level increases by a factor of 2 between $y/\delta = .6$ and $y/\delta = .05$. Why does the fluctuation level vary if we are measuring perturbations due to the same large scale eddy system?

A simple explanation for these observations can be suggested by considering the effect of the wall on the perturbation field. If no wall were present, the induced velocity field associated with vorticity at P' would be symmetrical about P' . When the wall is present, the induced velocity field of the image vorticity for P' must be added to the field directly due to P' . This will cause an increase of the induced velocities between P' and the wall and a decrease of the induced velocities beyond P' . This image effect may be the reason why the fluctuation level associated with the same large scale vorticity increases towards the wall.

So far we have managed to avoid specifying the extent of the sublayer. This has been a somewhat ambiguous question and has been subject to different interpretation by different authors. In Figure 7 the variation of the u' fluctuation and the turbulent shear stress \overline{puv} near the wall are shown for a boundary layer and a pipe flow. The variation of \overline{puv} has been calculated using the measured mean velocity profile and the fact that the total shear stress is essentially constant near the wall. As is customary, the data are presented in terms of the friction velocity $U_\tau = \sqrt{\tau_w/\rho}$ where τ_w is the friction at the wall and ρ is the density. In both cases, the peak of the u' fluctuation is found at $U_\tau y/\nu = U_\tau r/\nu = 15-20$. Some authors specify $U_\tau y/\nu \approx 12$ as the edge of the laminar sublayer and consider the region $12 < U_\tau y/\nu < 60$ to be some sort of transition region between the laminar sublayer and the fully developed turbulent part of the flow. The fact that the mean velocity profile is nearly linear up to $U_\tau y/\nu \approx 12$ seems to support this definition. On the other hand, at $U_\tau y/\nu \approx 12$, the turbulent shear stress is still only about 1/2 of the level of shear at the wall, and only asymptotically approaches the wall shear value somewhere around $U_\tau y/\nu \approx 100$ or $U_\tau r/\nu \approx 60$ according to Figure 7.

Viewing the region near the wall as a whole we can describe what is observed in the following general terms. Outside of the wall region, the turbulent shear stress and the u' fluctuation vary slowly compared to the variations that are found in the wall region. Entering the wall region the u' fluctuation first rises. In Figure 7, the fluctuation level is normalized in terms of the fluctuation level at the edge of the wall region. (It is more difficult to identify the edge of the wall region for the boundary layer case. This is because the variation of u' outside the wall region is much larger in the boundary layer case than in the pipe flow). Apparently, the fluctuation level increases more in Klebanoff's experiments than in Laufer's case. However, the fluctuation level in the sublayer should probably be compared with an extrapolation to the wall of the u' variation outside the sublayer. This would make a significant difference

in the case of the boundary layer and would suggest that the rise in fluctuation level in the boundary layer is not as great as it first appears to be. Approximately at the point where u' starts to rise, the shear stress starts to decrease slowly. The rapid decrease in u' is confined to the inner 25% of the wall region. In the theory given in this paper, the sublayer is the entire region between the wall and the fully developed turbulent part of the flow. There is no theoretical distinction between an inner "laminar" sublayer and a transition region although the rapid changes do primarily occur in the inner portion of the sublayer.

The physical picture of the large scale eddies containing most of the turbulent energy moving downstream at a velocity of the order of .8 of the free stream velocity U_1 is reminiscent of the physical picture of oscillations in a laminar boundary layer. In that case typical waves move downstream with a velocity $U_w \approx (2/3)U_1$ and have wave lengths of the order of $(2-5) \delta$. In the equations of motion for the perturbations in a laminar flow, the term representing the action of viscosity is negligible except in two limited regions of the boundary layer, the critical layer and the inner viscous layer close to the wall. We shall show that this inner viscous layer for fluctuations in a laminar boundary layer corresponds directly to the sublayer for a turbulent flow. Thus the sublayer is the region where the turbulent fluctuations in the shear flow are damped by viscosity.

The existence of a "dissipation layer" near the wall was first suggested by Townsend on the basis of a study of the turbulent energy balance in the boundary layer. He concluded that the bulk of the turbulent energy dissipation takes place by direct viscous action on the large eddies in a layer which he thought was "most probably in contact with the laminar sublayer". In the present theory we find that the sublayer itself is a dissipative region and that its structure is primarily determined by the large scale fluctuations in the turbulence.

4. EQUATIONS FOR THE FLUCTUATION FIELD

The equations of motion for the fluctuations in a turbulent field (Lin 1959, p.246) are obtained by subtracting the well known Reynolds equation for the mean flow from the complete Navier-Stokes equations. We restrict our attention to a steady flow in which the mean velocity only has a component parallel to the flow direction, so that $U = U(y)$ and $V = W = 0$, where U , V , and W are the three components of the mean motion. We will also assume that the statistical properties of the turbulent field such as $\overline{u^2}$ and \overline{uv} only vary with y . These assumptions are reasonably well satisfied by a two dimensional boundary layer flow or a pipe flow. Then if u , v , and w are the disturbance velocities the components of total velocity are $\underline{u} = U+u$, $\underline{v} = v$, $\underline{w} = w$, and the pressure is $\underline{p} = P + p$. We can then write down the three equations of motion for the fluctuating field

$$\begin{aligned}
 (1) \quad & \frac{\partial u}{\partial t} + U \frac{\partial u}{\partial x} + v \frac{dU}{dy} + u \frac{\partial u}{\partial y} + v \frac{\partial u}{\partial y} + w \frac{\partial u}{\partial z} = - \frac{1}{\rho} \frac{\partial p}{\partial x} + \nu \nabla^2 u + \frac{\partial}{\partial y} (\overline{uv}) \\
 (2) \quad & \frac{\partial v}{\partial t} + U \frac{\partial v}{\partial x} + u \frac{\partial v}{\partial x} + v \frac{\partial v}{\partial y} + w \frac{\partial v}{\partial z} = - \frac{1}{\rho} \frac{\partial p}{\partial y} + \nu \nabla^2 v + \frac{\partial}{\partial y} (\overline{v^2}) \\
 (3) \quad & \frac{\partial w}{\partial t} + U \frac{\partial w}{\partial x} + u \frac{\partial w}{\partial x} + v \frac{\partial w}{\partial y} + w \frac{\partial w}{\partial z} = - \frac{1}{\rho} \frac{\partial p}{\partial z} + \nu \nabla^2 w + \frac{\partial}{\partial y} (\overline{vw}) \\
 (4) \quad & \text{and the continuity equation } \frac{\partial u}{\partial x} + \frac{\partial v}{\partial y} + \frac{\partial w}{\partial z} = 0.
 \end{aligned}$$

In each equation the mean term on the right is the average of the three non-linear terms on the left. We are in fact going to neglect these non-linear terms but some justification for this step is certainly required. For instance the term $\frac{\partial}{\partial y} (\overline{uv})$ is zero at the wall and zero outside the sublayer, but reaches a peak value in the inner portion of the sublayer at about $U_\tau y/\nu \approx 10$, (See Figure 7). We can make this justification a posteriori by finding a solution without the non-linear terms and then comparing the magnitude of $\frac{\partial}{\partial y} (\overline{uv})$ with the linear terms that have been retained. At this point we will state the results. The acceleration term $\frac{\partial u}{\partial t}$ is the leading linear term. At the point where $U_\tau y/\nu \approx 10$, $\frac{\partial(\overline{uv})}{\partial y}$

is about 15% of $\sqrt{\left(\frac{\partial u}{\partial t}\right)^2}$. At the same point the linear convective terms such as $U(\partial u/\partial x)$ are about 40% of $\partial u/\partial t$. It is evident that the non-linear terms are significant though smaller than the linear terms. When the balance of terms is examined over the frequency spectrum it is found that at the low end of the frequency spectrum, at say 10 c.p.s., the maximum value of $\frac{\partial (\overline{uv})}{dy}$ may be comparable in magnitude to the terms that are retained. But linearization of the equations appears to be a reasonable first step towards a theory. Of course the non-linear terms would be essential in any theory of turbulence. But here the turbulent field at the edge of the sublayer is assumed to be known from the experiments. Our purpose is merely to represent the fluctuation field between the known field at the edge of the sublayer and the wall.

The fluctuation field can now be represented by a superposition of Fourier components, each component of which can be separately analyzed. The type of disturbance that will be used will be based on our interpretation of the experimental data. As we have already suggested one result of the analysis will be that the terms containing the viscosity are only significant in a narrow region near the wall. It is this region where the viscous terms are important, that we identify as the sublayer of the turbulent flow. It should be emphasized that we are not concerned with the energy balance of the frequency components as is the case for the study of oscillations in a laminar flow. No stability calculations are involved in the description of the sublayer.

5. SIMPLIFIED THEORY

A field of turbulence can be represented by a Fourier superposition of elementary plane vorticity waves. The velocity vector associated with a given vector wave number lies in a plane perpendicular to the wave vector. On the other hand, we have previously shown that most of the fluctuation energy near the wall is an induced field arising from vorticity distributed throughout the boundary layer. The type of elementary disturbance that is appropriate then depends on the nature of the large scale vorticity in the boundary layer, and not on the vorticity field at the edge of the sublayer.

Physically, one might expect the shearing action of the mean flow to stretch out vortex lines in the direction of the mean flow. There might then be a preference in the large scale motions for vortices nearly parallel to the wall. Since the root-mean-square w' fluctuation is approximately .7 of the root-mean-square u' fluctuation (Figure 6), some type of "three dimensional" disturbance would appear to be necessary. Accordingly, we have chosen to assume a simple form of oblique disturbance at the edge of the sublayer δ_s as shown in Figure 8. We might imagine this disturbance to be associated with a periodic vorticity normal to the direction ξ . Then the velocity q associated with this disturbance is in the ξ direction, rather than normal to the ξ direction as would be true for a shearing wave. The velocity q varies as $q = Q \cos (2\pi/\lambda_\xi)\xi$, where $w/u = \tan \theta$. As shown by the experimental data, the sublayer is very small and the scale of the energy containing eddies is large. Under these conditions, if we consider a disturbance of a particular wave length, the variation of the perturbation velocity with y in the vicinity of the sublayer can be neglected compared to the variation inside the sublayer.

This oblique disturbance is carried downstream with the velocity U_w in the x direction. Thus the wave length in the x direction $\lambda_x = \lambda_\xi / \cos \theta$. Introducing complex notation, we can write with $\beta = 2\pi f$.

$$u = \text{Re} \left\{ C_1 e^{i(k_x \cdot x - \beta t)} \right\}$$

$$w = \text{Re} \left\{ B_1 e^{i(k_x \cdot x - \beta t)} \right\}$$

where $U_w = \beta/k_x$, $\tan \theta = B_1/C_1$ and Re stand for Real Part. Similarly the fluctuating pressure field can be represented as

$$p = \text{Re} \left\{ p_1 e^{i(k_x \cdot x - \beta t)} \right\} \quad \text{where } p_1 \text{ is complex.}$$

Inside the sublayer, we have

$$u = \text{Re} \left\{ h(y) e^{i(k_x \cdot x - \beta t)} \right\}$$

$$w = \text{Re} \left\{ k(y) e^{i(k_x \cdot x - \beta t)} \right\}$$

and

$$v = \text{Re} \left\{ g(y) e^{i(k_x \cdot x - \beta t)} \right\}$$

with $u = v = w = 0$ at the wall $y = 0$.

Now close to the wall where $u \rightarrow 0$, and $v \rightarrow 0$, the convective terms in the equations of motion can be neglected. For instance, in the sublayer $\partial u / \partial x = ik_x \cdot u$, $\partial u / \partial t = -i\beta u$, so that

$$\frac{\left| U \frac{\partial u}{\partial x} \right|}{\left| \frac{\partial u}{\partial t} \right|} = \frac{U}{U_w}.$$

Also from the continuity equation $\frac{\partial v}{\partial y} = -\frac{\partial u}{\partial x} - \frac{\partial w}{\partial z}$ with

$$\frac{\partial u}{\partial x} = ik_x \cdot u, \quad \frac{\partial w}{\partial z} = ik_x \cdot w \cdot \tan \theta, \quad \text{so that } v = - \int_0^y ik_x \cdot u dy - \int_0^y ik_x \cdot w \tan \theta dy$$

$$\text{or } v = 0 \left(|k_x \cdot \frac{u}{2} (1 + \tan^2 \theta) \cdot y| \right).$$

Provided the angle θ does not approach 90° , $v = O(|k_x \cdot u \cdot y|)$.

This limitation on θ does not appear to be significant. We are interested in the u and v components at the wave number k_x as obtained in a one-dimensional spectral analysis. The wave number for the oblique disturbance $k_\xi = k_x / \cos \theta$ so that $k_\xi \rightarrow \infty$ as $\theta \rightarrow 90^\circ$. Since the energy spectrum for the fluctuation field falls off very rapidly with increasing frequency, the high frequency oblique waves where $\theta \rightarrow 90^\circ$ probably make a negligible contribution to the u and v fields. With $\frac{dU}{dy} = O\left(\frac{U}{y}\right)$, we have

$$\frac{\left|v \frac{\partial U}{\partial y}\right|}{\left|\frac{\partial u}{\partial t}\right|} = O\left(\frac{U}{U_w}\right).$$

Since $U_w \approx .8U_1$ for the large scale eddies the convective terms can be neglected for $y \rightarrow 0$. As we shall show later, the thickness of the viscous region for a disturbance of frequency f is

$$\delta_s = O\left(\sqrt{\frac{\nu}{f}}\right). \quad \text{Then } \frac{\partial^2 u}{\partial x^2} / \frac{\partial^2 u}{\partial y^2} = O\left(\frac{(2\pi)^2 f \cdot \nu}{U_w^2}\right). \quad \text{For any frequency of}$$

of interest only the derivatives with respect to y need be retained. The equations of motion can then be simplified to the following form

$$(5) \quad \frac{\partial u}{\partial t} + \frac{1}{\rho} \frac{\partial p}{\partial x} = \nu \frac{\partial^2 u}{\partial y^2}$$

$$(6) \quad \frac{\partial v}{\partial t} + \frac{1}{\rho} \frac{\partial p}{\partial y} = \nu \frac{\partial^2 v}{\partial y^2}$$

$$(7) \quad \frac{\partial w}{\partial t} + \frac{1}{\rho} \frac{\partial p}{\partial z} = \nu \frac{\partial^2 w}{\partial y^2} \quad \text{together with the continuity equation. It is}$$

evident that to this order of simplification there is no coupling between the u and w fluctuation fields and the u component can be solved for separately.

Again under the restriction that the disturbance angle θ does not approach 90° , it can now be shown that the terms in equation (6) are of higher order compared to the terms in equation (5). For instance

$$\frac{\partial v}{\partial t} = -i\beta v = 0 \left[(k_x \cdot \beta \cdot \frac{u}{2})(1 + \tan^2 \theta) \cdot y \right] \text{ so that } \frac{\left| \frac{\partial v}{\partial t} \right|}{\left| \frac{\partial u}{\partial t} \right|} = 0 \left(k_x \cdot \frac{y}{2} \right) (1 + \tan^2 \theta)$$

or a maximum of $O(k_x \delta_s)$ (provided θ is reasonably limited) at the edge of the viscous region.

$$\text{Now } k_x \delta_s = O\left(\frac{2\pi}{U_w} \sqrt{\nu f}\right) \text{ With } U_w = 1.25 \times 10^3 \text{ cm/sec, } k_x \delta_s = 3.3 \times 10^{-2}$$

at $f = 300$ c.p.s. This merely expresses the fact that near the wall v is of higher order than u . It also follows that $\frac{\partial p}{\partial y} \ll \frac{\partial p}{\partial x}$.

An important consequence is that the pressure field does not vary with y in the viscous region. We have,

$$\frac{\partial}{\partial y} \left(\frac{1}{\rho} \frac{\partial p}{\partial x} \right) = i k_x \frac{1}{\rho} \frac{\partial p}{\partial y} \text{ and since } \frac{1}{\rho} \frac{\partial p}{\partial y} = O\left(\frac{\partial v}{\partial t}\right)$$

$$\frac{\partial}{\partial y} \left(\frac{1}{\rho} \frac{\partial p}{\partial x} \right) = O(k_x^2 \cdot \beta \cdot \frac{u}{2} (1 + \tan^2 \theta) \cdot y)$$

$$\text{or finally } \frac{\frac{\partial}{\partial y} \left(\frac{1}{\rho} \frac{\partial p}{\partial x} \right)}{\frac{\partial}{\partial y} \left(\frac{\partial u}{\partial t} \right)} = O\left(k_x^2 \cdot \frac{[1 + \tan^2 \theta]}{2} \cdot y^2\right)$$

Similarly it can be shown that

$$\frac{\frac{\partial}{\partial y} \left[\frac{1}{\rho} \frac{\partial p}{\partial z} \right]}{\frac{\partial}{\partial y} \left[\frac{\partial w}{\partial t} \right]} = O\left(k_x^2 \frac{[1 + \tan^2 \theta]}{2} \cdot y^2\right)$$

Thus the pressure field associated with the disturbance is constant through the viscous region, since $k_x^2 \delta_s^2 \ll 1$.

To find the solution to equation (5), we represent the disturbance as the sum of two components, where $u = u_1 + u_2$. The component u_1 represents the disturbance velocity before account is taken of the direct wall effect. As previously discussed, we assume that the variation of u_1 with y in the vicinity of the viscous region is negligible compared to the variation of u that occurs inside the viscous region. Since the convective terms have been neglected u_1 is not affected by the mean flow and is constant throughout the viscous region. u_2 represents the disturbance velocity component directly associated with the wall friction. Thus, at the edge of the viscous region $u_2 \rightarrow 0$, and at the wall $u_2 = -u_1$. If we write equation (5) as

$$\frac{\partial(u_1 + u_2)}{\partial t} = -\frac{1}{\rho} \frac{\partial p}{\partial x} + \nu \frac{\partial^2(u_1 + u_2)}{\partial y^2}$$

then the equations for u_1 and u_2 throughout the viscous region are

$$\frac{\partial u_1}{\partial t} + \frac{1}{\rho} \frac{\partial p}{\partial x} = 0$$

$$\frac{\partial u_2}{\partial t} = \nu \frac{\partial^2 u_2}{\partial y^2}$$

where as we have already shown, $\frac{1}{\rho} \frac{\partial p}{\partial x}$ does not vary through the viscous region.* Substituting

$$u_2 = h_2(y) e^{i(k_x \cdot x - \beta t)}$$

we have $h_2'' + \frac{i\beta h_2}{\nu} = 0$ which has the simple solution

$$h_2 = -e^{-\left[1-i\right]\sqrt{\frac{\beta}{2\nu}} y}$$

so that finally $u = u_1 + u_2 = \text{Re} \left\{ C_1 \left[1 - e^{-\left[1-i\right]\sqrt{\frac{\beta}{2\nu}} y} \right] e^{i(k_x \cdot x - \beta t)} \right\}$

* This same separation of equation (5) was used by Prandtl (1921) in discussing oscillations in a laminar boundary layer.

It is evident that the region of rapid change in u is $O(\sqrt{\nu/f})$ as previously asserted so that the extent of the viscous region is different for each frequency, decreasing in size as the frequency is increased. In order to compare these results with experiment, we calculate

$$\overline{u^2} = \frac{1}{2} \operatorname{Re} \left[h(y) h^*(y) \right]. \quad \text{Introducing the dimensionless variable}$$

$$Y = \sqrt{\frac{\beta}{2\nu}} y, \text{ we find}$$

$$(8) \quad \frac{\overline{u^2}}{C_1^2/2} = 1 - 2e^{-Y} \cos Y + e^{-2Y}.$$

This function is shown in Figure 9. For each frequency component $\overline{u^2}/(C_1^2/2) \rightarrow 1$ at $Y \approx 5$. The rapid decrease of $\overline{u^2}$ occurs for $0 < Y < 2$. Entering the viscous region $\overline{u^2}/(C_1^2/2)$ first increases reaching a peak value at $Y = 2.2$. Examination of the details of the solution shows that this increase of disturbance level entering the viscous region arises because near the outer edge of the viscous region u_1 and u_2 have an in-phase component instead of being 180° out of phase as at the wall.

Figures 5 and 9 can now be used to calculate the variation of the root-mean-square fluctuation level u' near the wall. According to Figure 5, the energy spectra are similar between $y/\delta = .05$ and $y/\delta = .58$. Then the disturbance energy for each frequency outside of the viscous region is given by setting $C_1^2/2 = \overline{u^2}$ at $y/\delta = .05$ from Figure 5. For each frequency, the variation of $\overline{u^2}$ with y is obtained from Figure 9. The $\overline{u^2}$ spectra for various values of y can then be computed, and are shown in Figure 10. As y/δ increases, the spectra approach the spectrum outside of the sublayer. Integrating for each value of y/δ and taking the square root, we finally obtain the variation of u' near the wall. In Figure 11(a), the ordinate u'/u'_1 is the ratio of u' inside the viscous region to the value of u'_1 outside. According to the calculations, $u'/u'_1 \rightarrow 1$ at about $y/\delta = .035$. The rise in the experimental u' fluctuation level near the

wall appears to start for $.03 < y/\delta < .4$, but it is not possible to establish this point with any precision because of the variation of u' outside the sublayer. A comparison of Laufer's pipe data with similar theoretical calculations is shown in Figure 11(b). In both cases the theory correctly predicts the total extent of the sublayer, and also the fact that there is a rapid decrease of u'/u'_1 close to the wall. On the basis of these calculations, we feel justified in identifying the viscous region in the theory with the sublayer in the experiments. On the other hand, the rise in fluctuation level entering the sublayer is much greater than the small rise found in the theory. It should be noted that by $y/\delta = .01$, the ratio U_ℓ/U_w , which is a measure of the relative magnitude of the convective terms that have been neglected is approximately .6, increasing to .75 by $y/\delta = .035$. Thus the agreement between theory and experiment ought to be better near the wall.

As shown in Figure 10, there is a marked change in the spectral distribution approaching the wall. Most of the energy is taken from the largest scale motions resulting in a fairly flat spectrum close to the wall. One spectral measurement was also made by Klebanoff at $y/\delta = .0011$, deep in the sublayer. These measurements are also shown in Figure 10 where they can be compared with the calculated spectrum for $y/\delta = .0011$. Qualitatively, the measurements confirm the expectations of the theory. However, there is a significant difference in magnitude between theory and experiment at $y/\delta = .0011$. A somewhat different way of applying the theory suggests itself.

Since we expect theory to be better near the wall, we can calculate the spectra in the sublayer based on the experimental spectrum at $y/\delta = .0011$ rather than the spectrum outside of the sublayer. That is, using Figure 9, the variation of $C_1^2/2$ with f is chosen so that the theoretical and experimental spectra coincide at $y/\delta = .0011$. Then the corresponding spectra can be computed at other values of y/δ . The results are shown in Figure 12 and the corresponding variation of u'/u'_1 is shown

in Figure 11(a). Here of course, u'/u'_1 for theory and experiment have been set equal at $y/\delta = .0011$. The theoretical variation of u'/u'_1 is now in much better accord with the experiments in the inner part of the sublayer, at least up to $y/\delta = .005$. Beyond $y/\delta = .005$, the theoretical curve rapidly departs from the experimental data with the theory rising to a much higher value of u' outside the sublayer.

A comparison of the experimental spectrum at $y/\delta = .05$ and the theoretical spectrum at $y/\delta = .005$ (Figure 12) indicates that the higher fluctuation level at $y/\delta = .005$ is due to an increase in the energy in the large scale eddies. This is consistent with the theory in that at $y/\delta = .005$, all frequencies above $f = 600$ c.p.s. should still be outside of the viscous region. Therefore it seems probable that the spectra shown in Figure 12 are a better representation of the spectra close to the wall than the spectra in Figure 10.

While it is possible to determine the variation of $\overline{u^2}$ in the viscous region without specifying the way the disturbance energy varies with the angle θ , a knowledge of the three dimensional character of the field is necessary to determine $\overline{v^2}$. Suppose we consider the disturbance velocities u_θ and v_θ associated with an oblique disturbance at angle θ . Since equations (5) and (7) are identical in form and $\frac{1}{\rho} \frac{\partial p}{\partial z} = \left(\frac{1}{\rho} \frac{\partial p}{\partial x}\right) \tan\theta$, the relation $w_\theta = u_\theta \tan\theta$ holds throughout the viscous region. We can then readily find

$$v_\theta = \left[1 + \tan^2\theta\right] \operatorname{Re} \left\{ g(y) e^{i(k_x \cdot x - \beta t)} \right\}$$

so that

$$(9) \quad \overline{v_\theta^2} = \frac{2\pi f v}{U_w^2} \left(\frac{C_\theta}{2}\right)^2 \left[1 + \tan^2\theta\right]^2 T(Y)$$

$$\text{where } T(Y) = \left\{ \left(1 - 2e^{-Y} \cos Y + e^{-2Y}\right) + 2Ye^{-Y}(\cos Y - \sin Y) - 2Y + 2Y^2 \right\}$$

Here C_0 is the magnitude of u_0 at the edge of the viscous region. Since the problem of properly accounting for the distribution of the oblique disturbances will not be considered in this paper, we are not able to compute $\overline{v^2}$ from the theory.

However, some remarks about the application of the present theory to the determination of the $\overline{v^2}$ field can be made. The factor f in the equation for $\overline{v^2}$ shifts the $\overline{v^2}$ spectrum to higher frequencies as compared with the $\overline{u^2}$ spectrum. This filtering action is a fundamental aspect of the response of the sublayer to the $\overline{u^2}$ fluctuation field. Whereas the one dimensional $\overline{u^2}$ fluctuation field decreases monotonically from $f = 0$, the $\overline{v^2}$ spectrum at the edge of the sublayer should exhibit a maximum. That is, the $\overline{v^2}$ field close to the wall may have a preferred wave length.

There are two further difficulties in the theoretical determination of $\overline{v^2}$ which should be mentioned. In order to compute the total $\overline{v^2}$, the integration would have to be carried out to frequencies greater than 300 c.p.s. This cannot be done in a satisfactory way for the following reasons. First the variation of U_w with frequency at the higher frequencies is not known. Second a basic limitation is imposed by the form of disturbance assumed in the theory. We have assumed that for a given frequency the variation of the perturbation velocity with y in the vicinity of the viscous region can be neglected compared to the variation inside the very small viscous region. Since the thickness of the viscous region δ_s is given by $\delta_s = 0(\sqrt{\frac{\nu}{f}})$ the ratio of the eddy scale to δ_s is then $\frac{L}{\delta_s} \approx \frac{U_w}{\sqrt{f\nu}}$. At $f = 300$ c.p.s., $\frac{L}{\delta_s} \approx 150$. Above 300 c.p.s., U_w must necessarily decrease below $.8U_{1s}$, but there are insufficient measurements to establish the variation of U_w with f . (This point will be mentioned again in discussing the wall pressure fluctuations.) Suppose we adopt the artificial picture of an eddy of scale L , travelling along the wall with the average velocity of its center located at $y = L/2$. Then for $f = 5.5 \times 10^3$, $L/\delta_s \approx 25$. This guess suggests that while L/δ_s will decrease with

increasing frequency, it may still be large enough. However, at say $y/\delta = .008$, for a frequency of 5.5×10^3 , the distance from the wall y is of the same order as the eddy scale L and it is obvious that the variation of the perturbation velocity outside of the viscous region would have to be taken into account. Accordingly, the theory may have to be limited in its application to the \sqrt{v}^2 spectra below $f = 300$ c.p.s.

We also find that the determination of the shear stress depends on a knowledge of the distribution of oblique disturbances. According to the simplified theory

$$(\overline{uv})_\theta = \left[\frac{1 + \tan^2 \theta}{2} \right] \operatorname{Re} \{ g(y) h^*(y) \} \text{ from which we obtain}$$

$$(10) \quad (\overline{uv})_\theta = - \left[1 + \tan^2 \theta \right] \frac{c_\theta^2}{2} \frac{\sqrt{\pi f \nu}}{U_w} [S(Y)]$$

$$\text{with } S(Y) = \left[1 - 2e^{-Y} \cos Y + e^{-2Y} - 2Ye^{-Y} \sin Y \right]$$

We recall that

$$v = v_1 + v_2, \text{ where } \frac{\partial u_1}{\partial x} + \frac{\partial v_1}{\partial y} = 0$$

and $\frac{\partial u_2}{\partial x} + \frac{\partial v_2}{\partial y} = 0$, where we have set $v_1 = v_2 = 0$, at $y = 0$. At the edge of the viscous region for any frequency, $u_2 \rightarrow 0$, and $v_2 \rightarrow \text{constant}$. If we designate the constant by $v_{2\infty}$, then the shear stress at the edge of the viscous region is due to the coupling of u_1 and $v_{2\infty}$. The function $S(Y)$ is shown in Figure 13 together with $\sqrt{u^2} / (c_1^2/2)$.

It is evident that in the inner portion of the viscous region the relative variation of u' and \overline{uv} with y for each frequency component is similar to the overall variation of u' and \overline{uv} shown in Figure 7. The increase in the shear stress lags behind the increase in the fluctuation level. In both experiment and theory, at the peak of the u' fluctuation

\overline{uv} is $.7 \rightarrow .8$ of the shear stress outside the viscous region. However, the magnitude of \overline{uv} given by the simplified theory is definitely too low. This can be shown in the following way.

Sufficient data are given by Klebanoff to calculate the spectral variation of $\overline{uv}/u'v'$ at $y/\delta = .05$. The results of the calculations are shown in Figure 14. For comparison, the variation of $\overline{uv}/u'v'$ inside the viscous region according to the simplified theory is shown in Figure 15. Apparently the correlation coefficient does not reach high enough values in the viscous region at least at the lower frequencies. The convective terms that have been neglected in the simplified theory ought to play a significant role in controlling the phase angle between u and v . Therefore this deficiency of the theory is not surprising.

Again the factor \sqrt{f} shifts the \overline{uv} spectrum to higher frequencies as compared with the u^2 spectrum but not as much as for the v^2 spectrum. Consequently the high frequency limitations on the theory that have already been discussed should not be so serious. But in any case, a computation of \overline{uv} would have to account for the three dimensional nature of the disturbance field.

6. MICROSCALES

Important changes in the dissipation derivatives or microscales occur on entering the sublayer. Here we will consider two of these derivatives which can be discussed, at least to a limited extent, using the simplified theory. The longitudinal microscale can be written as

$$(11) \quad \overline{\left(\frac{\partial u}{\partial x}\right)^2} = k_x^2 \frac{1}{2} \operatorname{Re} \left\{ h(y) \cdot h^*(y) \right\} = \frac{(2\pi)^2 f^2}{U_w^2} (C_1^2/2)$$

While there are no data in general for the variation of the disturbance velocity U_w with f above $f = 300$ c.p.s. a first guess for this variation can be made at $y/\delta = .05$. For separation distances $\leq .5$ cm the autocorrelation and longitudinal correlation curves of Klebanoff appear to coincide. This would suggest that $U_w = U_\ell$ for $L = .5$ cm. or $f \approx 2 \times 10^3$ c.p.s. Previously, we have set an upper limit of $f = 300$ c.p.s. for $U_w = .8U_1$. We assume then that the disturbance velocity varies linearly from $.8U_1$ at $f = 300$ to $U_w = U_\ell$ at 2000 c.p.s. Above $f = 2000$ c.p.s., U_w is set equal to U_ℓ . Integrating, we find $\frac{\delta}{U_1} \overline{\left(\frac{\partial u}{\partial x}\right)^2} = 5.8$

which compares with a value of 5.5 from the experiment. Deep in the sublayer the experimental value for $\overline{\left(\frac{\partial u}{\partial x}\right)^2}$ increases by about a factor of 2, but the uncertainty about the variation of U_w with f is too great to proceed with any theoretical calculations in this region.

The microscale transverse to the wall can be written as

$$(12) \quad \overline{\left(\frac{\partial u}{\partial y}\right)^2} = \frac{1}{2} \operatorname{Re} \left\{ h'(y) \cdot h'^*(y) \right\} \text{ which becomes}$$

$$\overline{\left(\frac{\partial u}{\partial y}\right)^2} = \frac{2\pi f}{v} \left(\frac{C_1}{2}\right)^2 e^{-2\sqrt{\frac{\beta}{2v}} y} \quad \text{Outside the sublayer, at}$$

$y/\delta \leq .05$, we have assumed a form of disturbance where $\frac{\partial u}{\partial y} = 0$, where in reality $\frac{\partial u}{\partial y}$ is small but not zero outside the viscous region. The experimental variation of $\frac{\delta^2}{2U_1^2} \overline{\left(\frac{\partial u}{\partial y}\right)^2}$ is shown in Figure 16. Approaching

the wall, there is a very rapid increase in the gradient normal to the wall. A rapid increase in $(\frac{\partial u}{\partial y})^2$ is also predicted by the theory. In fact, according to equation (12), $(\frac{\partial u}{\partial y})^2$ will be a maximum at the wall. Calculations have been carried out at several points in the inner part of the sublayer based on the measured spectrum at $y/\delta = .0011$, and the results are shown in Figure 16. It is evident that the simplified theory underestimates the value of $(\frac{\partial u}{\partial y})^2$ at $y/\delta = .005$, the inner limit of the experimental measurements. A possible reason for this discrepancy can be suggested. The large gradients in u in the simplified theory are confined to the region very close to the wall. Experimentally, as shown in Figure 11, substantial gradients in u are found over a much greater extent of the sublayer. We might anticipate that the simplified theory would underestimate $(\frac{\partial u}{\partial y})^2$ away from the wall.

The much greater experimental value of $(\frac{\partial u}{\partial y})^2$ as compared with $(\frac{\partial u}{\partial x})^2$ does not reflect a distortion of the small scale eddies. For instance at $y/\delta = .005$, the theoretical spectrum for $(\frac{\partial u}{\partial y})^2$ shows that practically all the contribution to $(\frac{\partial u}{\partial y})^2$ comes from frequencies < 300 c.p.s.

7. THE PRESSURE FIELD

Extensive measurements of the pressure fluctuations at the boundaries of turbulent flows have been made by Willmarth (1958,1959). He found that the major contribution to the pressure fluctuations comes from large scale fluctuations. Of particular interest, his space-time correlation measurements show that the pressure pattern is convected downstream with a speed of $.82U_1$. This observation is in good agreement with the present theory where the large scale fluctuations move downstream at the mean velocity of the middle region of the boundary layer. In fact measurements of the wall pressure field may provide a means of experimentally establishing the variation of disturbance velocity with frequency for the higher frequencies in the sublayer. Corcos and Winkle (1960) have found that by making a spectral resolution of the longitudinal space-time correlation a functional relationship between convective velocity and frequency can be found. As we would expect theoretically the higher frequencies are convected more slowly than the low frequencies. However, theoretical calculation of the spectrum and the magnitude of the pressure fluctuations at the boundary layer is another matter.

The pressure fluctuations in a turbulent shear flow may be much larger than in a field of isotropic turbulence at comparable turbulent fluctuation levels. This is the case near the edge of the laminar sublayer in a turbulent boundary layer. Very large pressure fluctuations are associated with the linear terms in the equations of motion. Just outside of the sublayer, retaining all the linear terms, equation (1) becomes

$$(13) \quad \frac{\partial u}{\partial t} + U \frac{\partial u}{\partial x} + v \frac{dU}{dy} = - \frac{1}{\rho} \frac{\partial p}{\partial x}$$

The fluctuation field at the edge of the sublayer is now represented by a superposition of Fourier components. Using the same notation as in the previous sections, we can write equation (13) as

$$p_1 = \rho U_w \left\{ h(y) \left[1 - \frac{U_\ell}{U_w} \right] - \frac{g(y)}{ik_x} \frac{d\left(\frac{U_\ell}{U_w}\right)}{dy} \right\} e^{i(k_x x - \beta t)}$$

Then the spectral variation of $\overline{p^2}/\rho^2$ is given by

$$(14) \quad \frac{\overline{p^2}}{\rho^2} = F \frac{\overline{u^2}}{u^2} [U_w - U_\ell]^2 + \frac{F \overline{u^2} U_w^2}{(2\pi)^2 F^2} \left[\frac{dU_\ell}{dy} \right]^2 - \frac{U_w}{\pi F} [U_w - U_\ell] \frac{dU_\ell}{dy} F \overline{(iu)v}$$

In isotropic turbulence, $U_w = U_\ell$, $\frac{dU_\ell}{dy} = 0$, and the pressure field due to these linear terms vanishes. At high frequencies, $U_w = U_\ell$ and the first and third terms do not contribute to the pressure field. However, most of the contribution to the pressure fluctuations comes from the low frequencies and these terms are important. The spectral functions $F \frac{\overline{u^2}}{u^2}$ and $F \frac{\overline{v^2}}{v^2}$ have been measured at the edge of the sublayer at $y/\delta = .05$, and can be directly used in calculating $\overline{p^2}/\rho^2$. An additional assumption must be made in order to determine $F \overline{(iu)v}$.

For a given frequency component, the shear correlation coefficient $\overline{uv}/u'v' = \cos \phi$ where ϕ is the phase angle between the u and v velocities. If we represent u on the positive real axis in the complex plane, then a negative correlation coefficient indicates that v is either in the second or third quadrants since ϕ must lie between 90° and 270° . Now according to the simplified theory, $180^\circ < \phi < 270^\circ$ throughout the viscous region (measuring ϕ counterclockwise from u). Assuming then that v lies in the third quadrant the correlation spectrum $F \overline{(iu)v}$ can be computed using the variation of the experimental phase angle ϕ with frequency as given in Figure 14. That is if γ is the phase angle between iu and v , then $\cos \gamma = \sin \phi$, and $F \overline{(iu)v}$ is negative making the third term in equation (14) positive. The resulting spectrum for $\overline{p^2}/\rho^2$ is shown in Figure 17 where we have set $U_w = .8U_1$. If v lies in the second instead of the third quadrant, then the sign of $F \overline{(iu)v}$ is reversed although the magnitude is the same. In that case the pressure fluctuation spectrum would be represented by the lower boundary of the cross hatched region in Figure 17. The second term of equation 14, $\frac{\overline{v^2}}{k_x^2} (dU_\ell/dy)^2$ is also given in Figure 17 to indicate what might be expected from the linear theory at the higher frequencies.

It is interesting to compare these calculations with the pressure spectrum for an isotropic field, where the pressure fluctuations are due to the non-linear terms. Batchelor (1956, p. 181) has given an expression for the pressure fluctuations in an isotropic field in terms of the three dimensional energy spectrum. The first step then is to find an appropriate energy spectrum for this flow. Since the Reynolds number of the turbulence is large, the one dimensional spectrum F_u^2 at $y/\delta = .05$ can be fitted by the function

$$F_u^2 = \frac{L_x}{U_l} \left[\frac{4}{1 + 4\pi^2 \frac{F_u^2 L_x^2}{U_l^2}} \right]$$

where L_x is the longitudinal integral scale (Dryden 1943). Then using the transformation between the one and three dimensional energy spectra for isotropic turbulence, the three dimensional spectrum $P(k)$ can be computed using Batchelor's theory where

$$\int_0^\infty P(k) dk = \overline{p^2}/\rho^2. \text{ Finally, the one dimensional pressure}$$

spectrum F_p^2 , where we represent $\overline{p^2}/\rho^2$ by \tilde{p} , can be obtained from

$$F_p^2 = \int_{k_x}^\infty \frac{P(k)}{k} dk \text{ and is also shown in Figure 17}$$

(transformed to a frequency spectrum). The values given are appropriate to an isotropic field with each component equal to u' . It is evident that at the edge of the sublayer, the linear terms are the main source of the pressure field.

The present theory provides a clear basis for having a pressure field at the boundary. For each frequency component $\frac{\partial}{\partial y}(\frac{\partial p}{\partial x}) \approx 0$ across the viscous layer. Even though the fluctuation components vanish at the wall,

the pressure field does not vanish with them. This is in contrast to an isotropic pressure field where $\overline{p'^2}/\rho^2 \propto (u')^4$. It would then follow that the pressure fluctuations at the boundary should be of the same order as the pressure fluctuations at the edge of the sublayer. Using boundary layer parameters appropriate to Klebanoff's experiment, Willmarth's wall measurements are also shown in Figure 17. Integrating the spectra in Figure 17, and taking the square root, we have $\frac{\overline{p'}}{\rho U_\tau^2} = 19 \rightarrow 30$, for the linear terms, 3.7 for the isotropic field and 2.4 from Willmarth. It is apparent that the wall pressure field is much smaller than what would be expected from the present theory. Perhaps the non-linear terms that have been neglected are essential for the computation of the pressure fluctuations in the sublayer. In part this may be because a major contribution to the pressure field comes from the lowest frequencies and at these frequencies the non-linear terms are relatively more important.

8. TURBULENCE PRODUCTION

A good deal of significance has been attached to the experimental observation that the flow of turbulent energy from the mean flow to the fluctuating field reaches a maximum in the sublayer. This observation has suggested the following physical picture. Adjacent to the wall, there is a laminar flow. Moving out from the wall a region of instability develops because of the high disturbance level of the turbulence in the boundary layer. Along the outer edge of the "laminar flow", transition to turbulence occurs, producing a region of intense turbulence and of course "turbulence production". Finally going still further from the wall, the flow settles down to a reasonably well behaved fully turbulent flow.

In terms of the theory given in this paper, the peak in turbulence production does not suggest such a physical model. Furthermore if we start with the condition that the total shear stress for the mean flow be constant across the sublayer, then we can readily show that there will be a peak in turbulence production where

$$-\rho \overline{uv} = \mu \frac{dU}{dy}$$

The total shear is $-\rho \overline{uv} + \mu \frac{dU}{dy} = \tau_w = \text{Constant}$.

The turbulence production (Pr) is given by

$$(Pr) = -\rho \overline{uv} \frac{dU}{dy} = (\tau_w - \mu \frac{dU}{dy}) \frac{dU}{dy}$$

Then
$$\frac{\partial}{\partial y} (Pr) = \tau_w \frac{d^2U}{dy^2} - 2\mu \frac{dU}{dy} \left(\frac{d^2U}{dy^2} \right) = 0,$$

and we have $\mu \frac{dU}{dy} = \frac{\tau_w}{2}$ for maximum production. This result is confirmed by the experiments of Klebanoff and Laufer. Thus while the region of maximum turbulence production is important for determining the structure of the turbulence, it need not be given any phenomenological significance.

Generally speaking in the fully developed part of the boundary layer, the energy flows from the mean flow into the large scale eddies. At $y/\delta = .05$, from Klebanoff, 70% of the shear stress is found between

$0 < f < 300$, which compares with 80% of $\overline{u^2}$ below $f = 300$. This situation is altered in the sublayer. At the point where $\mu \frac{dU}{dy} = \frac{\tau_w}{2}$ the loss in turbulent shear stress has come from the large scale eddies. This means that the turbulence production goes into ever smaller eddies as the wall is approached. Therefore the region of maximum turbulence production may not be important in determining the energy balance of the large scale, energy containing eddies in the boundary layer.

9. LAMINAR-TURBULENT TRANSITION IN STRONG TURBULENCE

The most satisfactory correlation of the experimental data for the Reynolds number of boundary layer transition in strong free stream turbulence has been given by Taylor (1936). Taylor derived his transition parameter on the assumption that the fluctuating pressure gradients of the turbulence cause momentary separation of the laminar boundary layer, thereby leading to transition. In recent years, detailed investigations of transition have been carried out by Schubauer and Klebanoff (1955). In no case do they find any experimental support for the idea that momentary separation is involved in the transition phenomena.

The flow near the wall of a laminar boundary layer with a strong free stream turbulence is in many respects similar to the flow in the sublayer of a turbulent flow. The scale of the free stream turbulence is in general large compared with the thickness of the laminar boundary layer. The free stream turbulence moves downstream with the free stream flow, and therefore at a disturbance velocity much larger than the local mean velocities in the boundary layer near the wall. In accordance with the present theory, we should expect to find a "sublayer" of the eddies of the free stream turbulence in a small region close to the wall. The neglected non-linear terms, which are of concern in the treatment of the sublayer of a turbulent flow, are of no importance in this case.

The present theory has been applied to the experimental conditions given by Dryden (1936). These data are at a transition Reynolds number based on the displacement thickness δ^* of $R_{\delta^*} \approx 500$, which appears to be the lowest transition Reynolds number to be found in the literature. This is very close to the minimum critical Reynolds number of $R_{\delta^*} = 400$ of the small disturbance stability curve for laminar boundary layer oscillations. Accordingly, it should not be necessary to take into account the amplification of the disturbance level in the boundary layer in this case.

Liepmann, Laufer and Liepmann (1951) have measured the energy spectrum for the free stream turbulence in a wind tunnel under experimental conditions reasonably close to those of Dryden. We estimate $L_x/U_1 \approx 1 \times 10^{-3}$ for Dryden where $L_x/U_1 = .9 \times 10^{-3}$ for Liepmann. Thus Liepmann's spectrum can be used to calculate the "sublayer" for Dryden's experimental point. It is found that the disturbances due to the free stream turbulence are damped down by viscosity in a "sublayer" approximately .15 cm thick. The close similarity between the physical picture for the sublayer of a turbulent flow and the "sublayer" of the free stream turbulence in a laminar boundary layer is shown in Figure 18. The scale corresponding to 50% of the u^2 energy is shown in each diagram. It seems clear that the physical model used by Taylor, in which the mean boundary layer responds to the pressure gradients associated with the turbulence is not applicable to the description of the laminar boundary layer in a strong free stream turbulence.

Nevertheless, Taylor's parameter does appear to correlate the available experimental data. We would now like to show that by introducing an additional physical assumption we can obtain a transition parameter very similar to that of Taylor's. No attempt will be made to justify this assumption here although it has led to reasonable results in some previous work (Lin, 1955, p.90)

We assume that the onset of transition depends on the relative amplitude of the Reynolds stress associated with the turbulent fluctuations and the shear in the mean flow. This is, we adopt as a rough criterion for the onset of transition, the requirement that

$$-\rho \overline{uv} = f(Re_{tr}) \cdot \mu \frac{U}{\delta}$$

From the simplified theory, the shear stress outside the "sublayer", is of the form

$$-\rho \overline{uv} \propto \rho (u')^2 \frac{\sqrt{f} \sqrt{v}}{U_w}$$

Here $U_w = U_1$, the free stream velocity. The frequency f can be replaced by $f = U_1/L_e$ where L_e represents the "scale" of the turbulence. Then

$$- \rho \overline{uv} \propto \rho (u')^2 \frac{\sqrt{v}}{\sqrt{U_1 \cdot L_e}}$$

Now the thickness of the laminar boundary layer at transition is

$$\delta_{tr} \propto \sqrt{\frac{x_{tr} v}{U_1}}$$

Substituting, we have

$$\rho (u')^2 \cdot \frac{\sqrt{v}}{\sqrt{U_1 \cdot L_e}} = f_1 (Re_{tr}) \cdot \frac{\mu \cdot U_1^{3/2}}{\sqrt{v x_{tr}}}$$

Finally, we obtain

$$\left(\frac{u'}{U_1}\right) \left(\frac{x_{tr}}{L_e}\right)^{1/4} = f_1 (Re_{tr})$$

Taylor's parameter is

$$\left(\frac{u'}{U_1}\right) \left(\frac{x_{tr}}{L_y}\right)^{1/5} = f_2 (Re_{tr}) \text{ where } L_y \text{ is the lateral integral}$$

scale of the free stream turbulence. The available transition data are too scattered to make it possible to distinguish between a $1/4$ or $1/5$ power variation with x_{tr}/L . From the point of view of correlating the experimental data either parameter would be equally effective although Taylor's parameter is based on the assumption that transition is caused by the small eddies, whereas for the new parameter it is assumed that transition is caused by the large eddies.

10. CONCLUDING REMARKS

The vorticity field responsible for the turbulent fluctuations in a boundary layer or similar shear flow is swept along with the velocity of the fluid elements. The velocity fluctuation field associated with this vorticity field is altered by the wall in two ways. The effect of the boundary condition $v = 0$ is to increase the magnitude of the wall velocity fluctuations u and w in the plane of the wall. The induced velocity at the wall associated with each element of vorticity is doubled by the image vortex element required to cancel v at the wall. This form of "wall effect" extends across the boundary layer and beyond into the potential flow. As a result of the boundary conditions $u = w = 0$ the turbulent velocity fluctuations are directly damped down by viscosity in a thin layer, the sublayer.

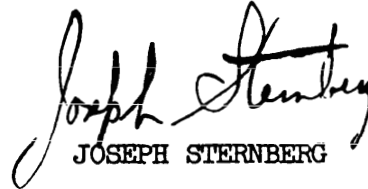
The equations of motion for the turbulent velocity and pressure fluctuations are applied only in this narrow viscous region. The aim of the theory is to say, in detail, how a known turbulent field dies out to nothing at the wall.

A simplified form of the theory is given in this paper. Only the leading terms in the differential equations are retained. Furthermore while the three dimensional character of the fluctuation field is recognized and introduced at any early stage the calculations are not carried far enough to make the three dimensionality important.

The same basic approach can be used to develop a more accurate description of the sublayer. The linear convective terms can be retained in the equations and solutions are being obtained using computing machines. Also the influence of the distribution of oblique disturbances on the fluctuation field is being explored. It is hoped to report the results of these studies in the future.

Calculations with the theory could be applied to such quantities as $\overline{v^2}$ and \overline{uv} if the variation of disturbance velocity with frequency at the higher frequencies could be established. This might be done from space-time correlation measurements of wall pressure fluctuations.

Finally there are related problems in which the present approach may be useful. We have already shown that the theory applies to the "sublayer" of the free stream turbulence in a laminar boundary layer. A similar approach might be useful in the description of turbulent heat and mass transfer.


JOSEPH STERNBERG

ACKNOWLEDGMENT

The author would like to thank Miss Joan Bartos for her help in performing the many calculations required for this report.

REFERENCES

1. Batchelor, G. K. "The Theory of Homogeneous Turbulence", Cambridge University Press, Cambridge, England (1956) p.181.
2. Corcos, G. M. and von Winkle, W. "Measurements of the Pressure Field at the Boundary of a Fully Developed Turbulent Pipe Flow", Bull. Am. Phys. Soc. Series II, Vol. 5, March 4, 1960.
3. Dryden, H. L. "Air Flow in the Boundary Layer Near a Plate", NACA Report 562 (1936).
4. Dryden, H. L. "A Review of the Statistical Theory of Turbulence", Quart. Appl. Math., 1, 7 (1943).
5. Einstein, H. A. and Li, H. "The Viscous Sublayer Along a Smooth Boundary", Proc. Am. Soc. Civ. Eng., Paper 945, (1956).
6. Fage, A. and Townend, H. C. H. "An Examination of Turbulent Flow With an Ultramicroscope", Proc. Roy. Soc. (London), 135, 656, (1932).
7. Favre, A. J., Gaviglio, J. J. and Dumas, R. J. "Space-time Double Correlations and Spectra in a Turbulent Boundary Layer", 2, 313 (1957).
8. Favre, A. J., Gaviglio, J. J. and Dumas, R. J. "Further Space-time Correlations of Velocity in a Turbulent Boundary Layer", 3, 344, (1958).
9. Hanratty, T. J. "Turbulent Exchange of Mass and Momentum With a Boundary", Am. Inst. Chem. Eng., 2, 359, (1956).
10. Klebanoff, P. S. "Characteristics of Turbulence in a Boundary Layer With Zero Pressure Gradients", NACA Tech. Note 3178, (1954).
11. Laufer, J. "Investigations of Turbulent Flow in a Two-Dimensional Channel", NACA Tech Note 2123 (1950).
12. Laufer, J. "The Structure of Turbulence in Fully Developed Pipe Flow", NACA Tech. Note 2954 (1953).
13. Liepmann, H. W., Laufer, J. and Liepmann, Kate "On the Spectrum of Isotropic Turbulence", NACA Tech. Note 2473 (1951).
14. Lin, C. C. "On Taylor's Hypothesis and the Acceleration Terms in the Navier-Stokes Equations", Quart. Appl. Math., 10, 295, (1953).
15. Lin, C. C. "The Theory of Hydrodynamic Stability", Cambridge University Press, Cambridge, England, (1955) p. 90.

REFERENCES (cont'd)

16. Lin, C. C., Editor "High Speed Aerodynamics", Princeton University Press, Princeton, New Jersey, (1959), Vol. V, p. 246.
17. Prandtl, L. "Bemerkungen über die Entstehung der Turbulenz". Z. angew. Math. u. Mech., 1, p. 431 (1921).
18. Schubauer, G. B. and Klebanoff, P. S. "Contributions on the Mechanics of Boundary Layer Transition", NACA Tech. Note 3489 (1955).
19. Taylor, G. I. "Conditions at the Surface of a Hot Body Exposed to the Wind", Brit. Adv. Com. Aeronaut. Repts. and Mem. 272 (1916).
20. Taylor, G. I. "Note on the Distribution of Turbulent Velocities in a Fluid Near a Solid Wall", Proc. Roy. Soc. (London), 135, 678, (1932).
21. Taylor, G. I. "Statistical Theory of Turbulence", Part V. Proc. Roy. Soc. (London) 156, 307, (1936).
22. Taylor, G. I. "The Spectrum of Turbulence", Proc. Roy. Soc. (London) 164, 476 (1938).
23. Townsend, A. A. "The Structure of the Turbulent Boundary Layer", Proc. Cambridge Phil. Soc., 47, 375, (1951).
24. Willmarth, W. W. "Wall Pressure Fluctuations in a Turbulent Boundary Layer", NACA Tech. Note 4139 (1958).
25. Willmarth, W. W. "Space-Time Correlations and Spectra of Wall Pressure in a Turbulent Boundary Layer", NASA Memo 3-17-59W, (1959).

$y/\delta = .58$ From Klebanoff
(Normalized)

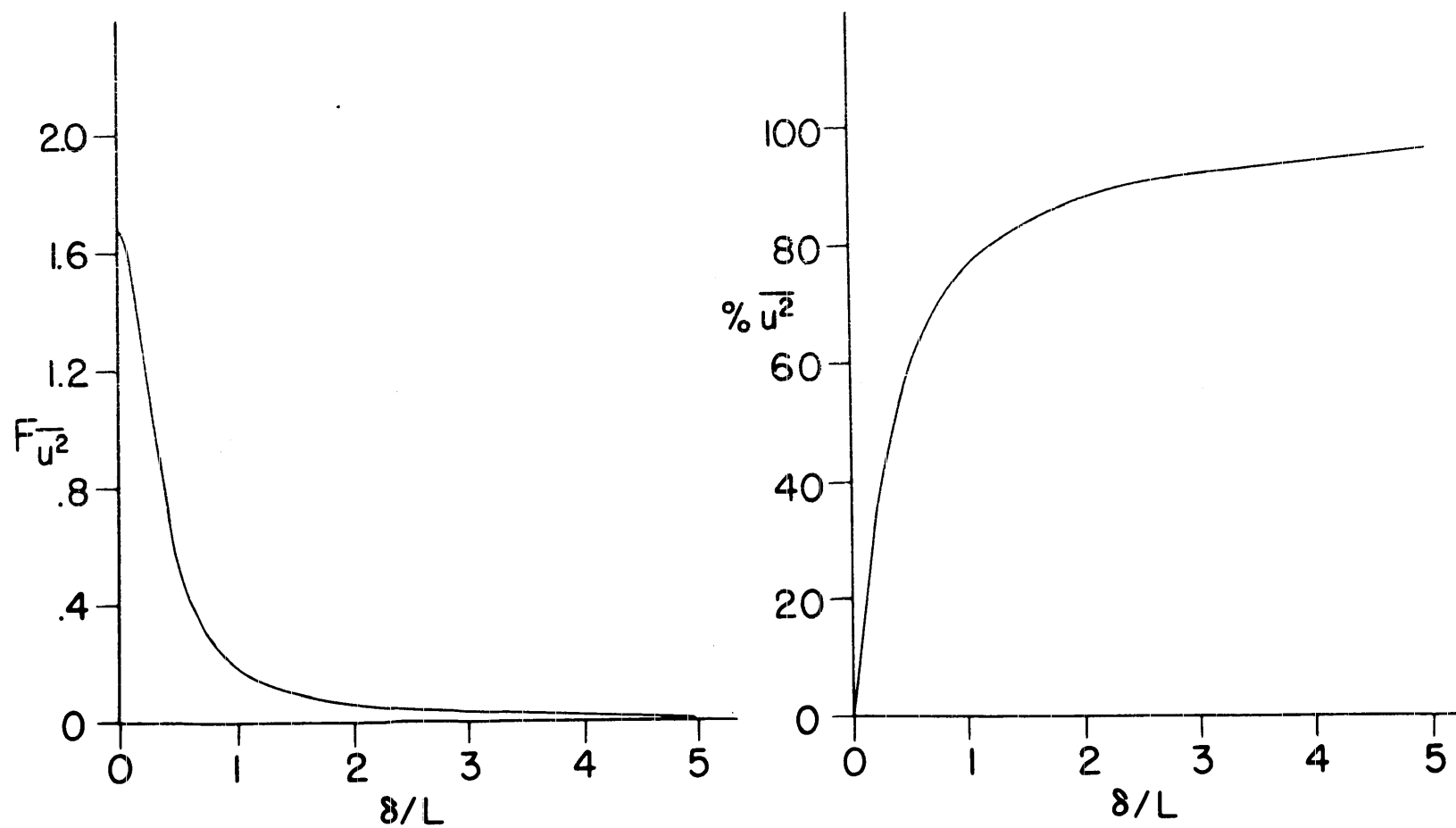


Figure 1. Typical Boundary Layer Energy Spectrum

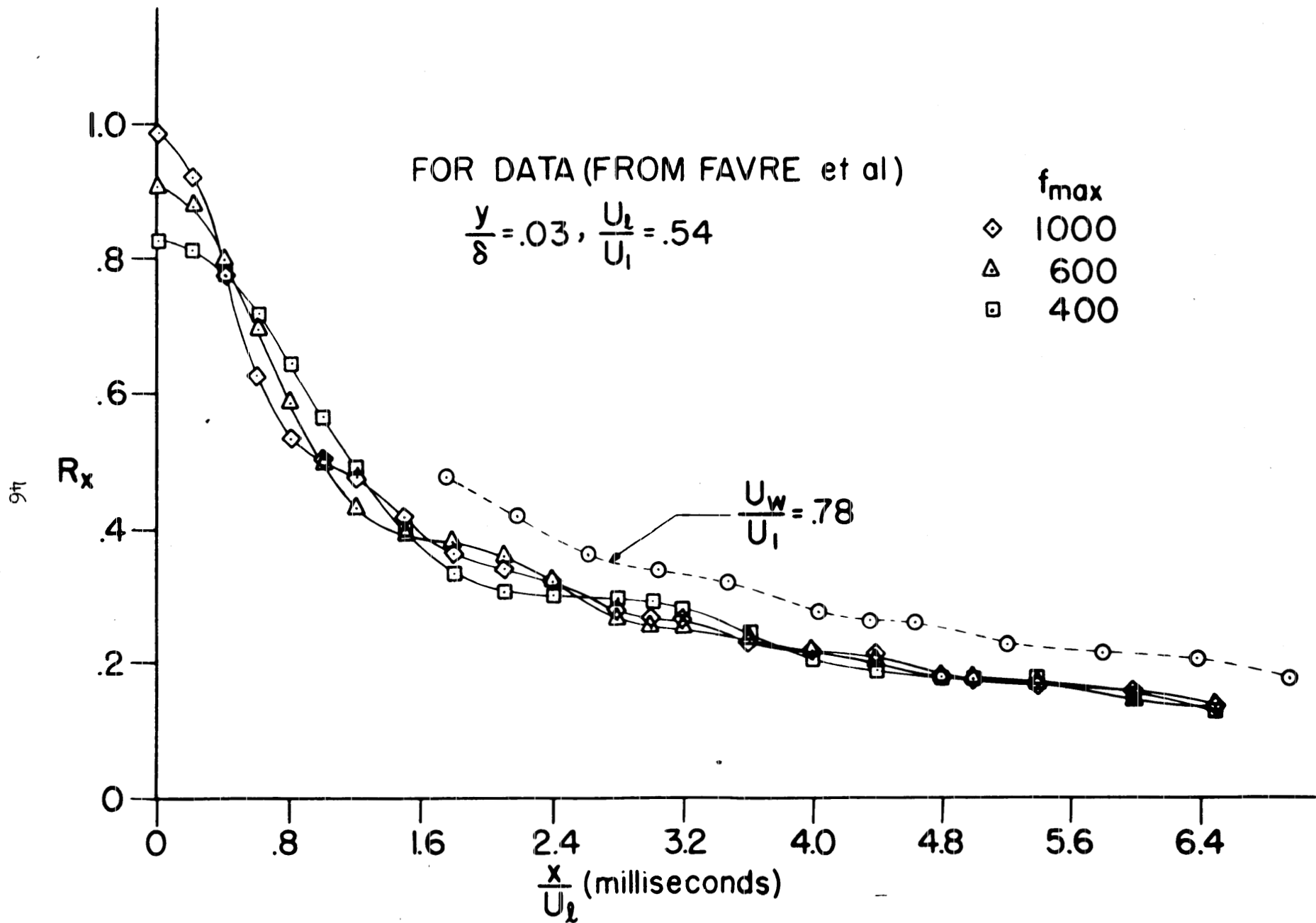


Figure 2. Effect of Frequency Cutoff and Disturbance Velocity on Auto-correlation Coefficient.

- Autocorrelations
- Longitudinal Space Correlations

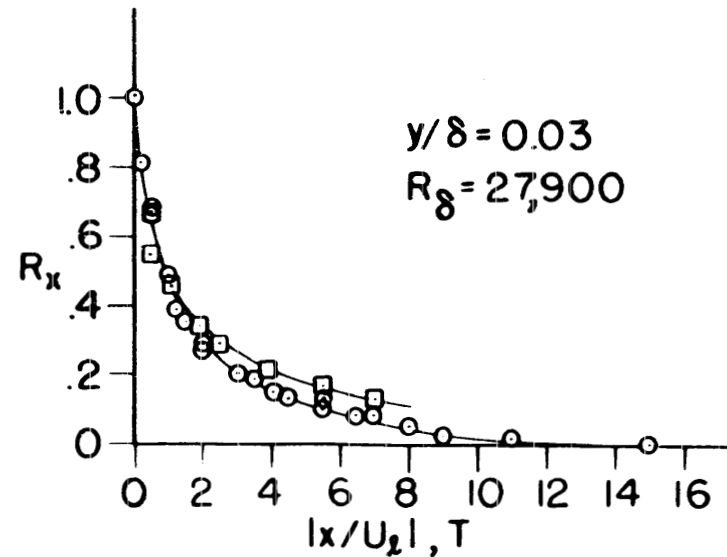
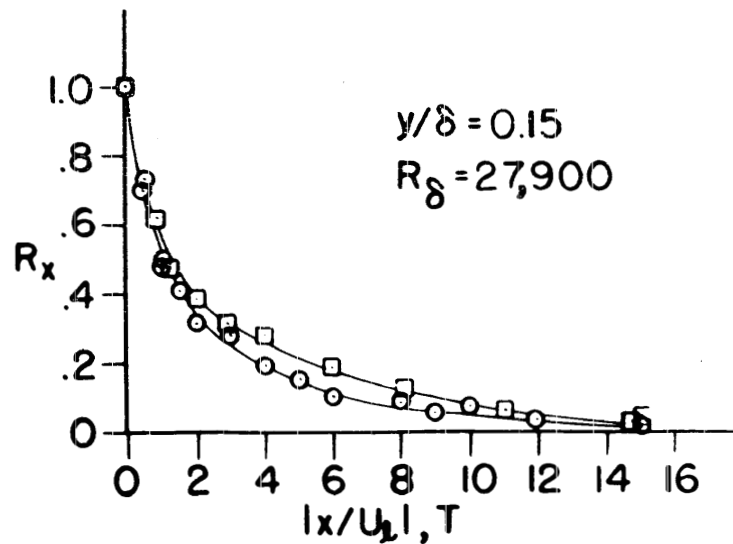
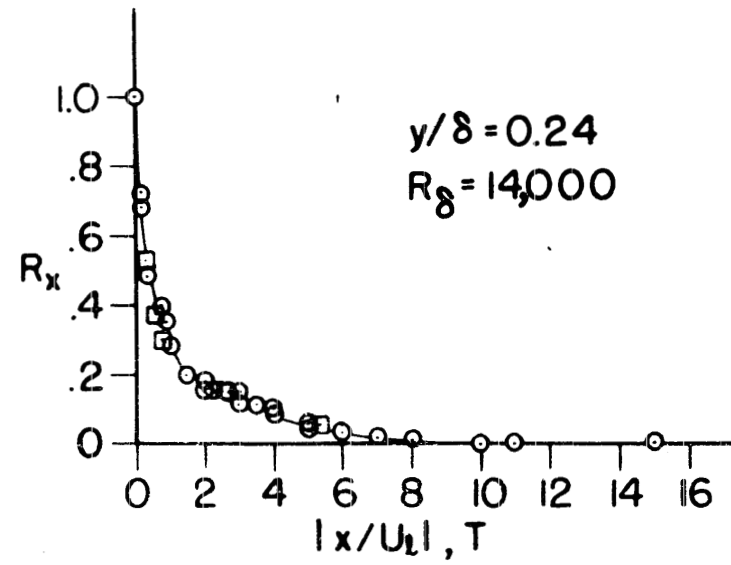
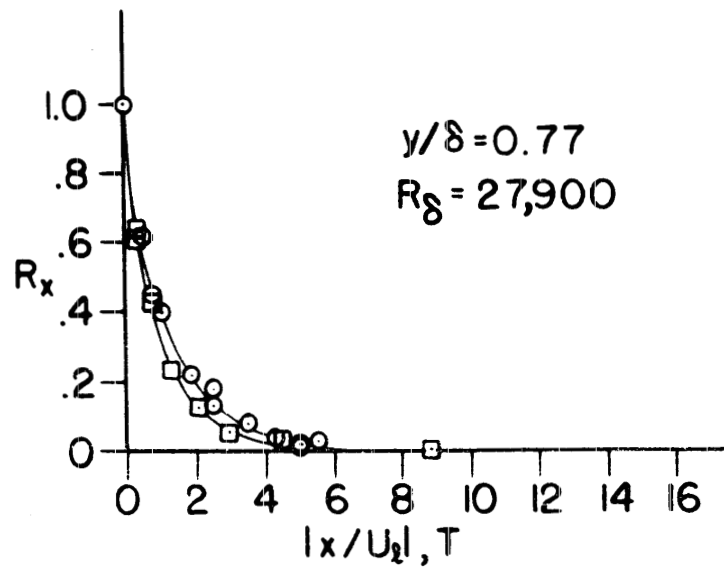


Figure 3. Comparison of Autocorrelation and Longitudinal Correlation Coefficients From Favre.

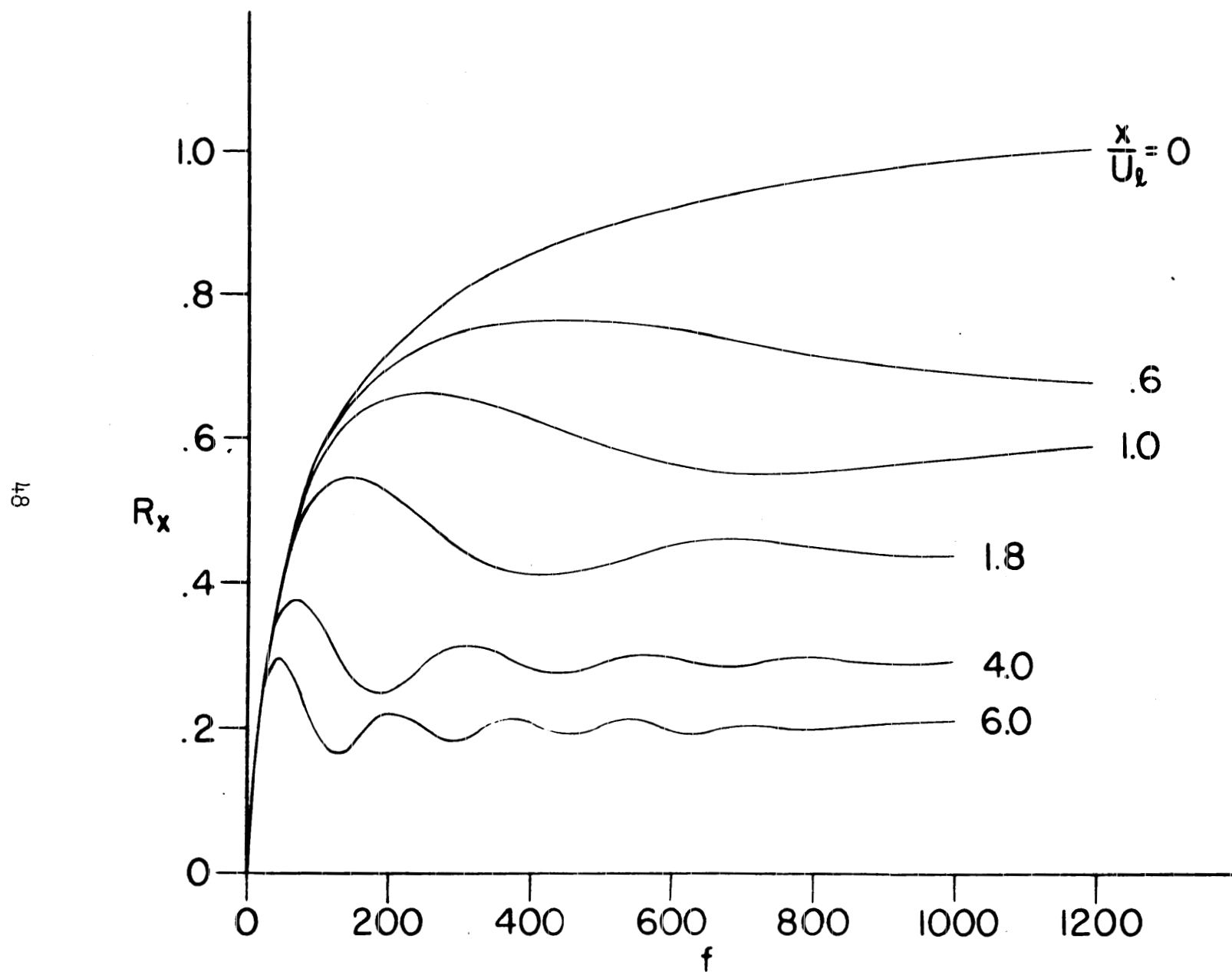


Figure 4. Autocorrelation Functions for Klebanoff Boundary Layer Data.

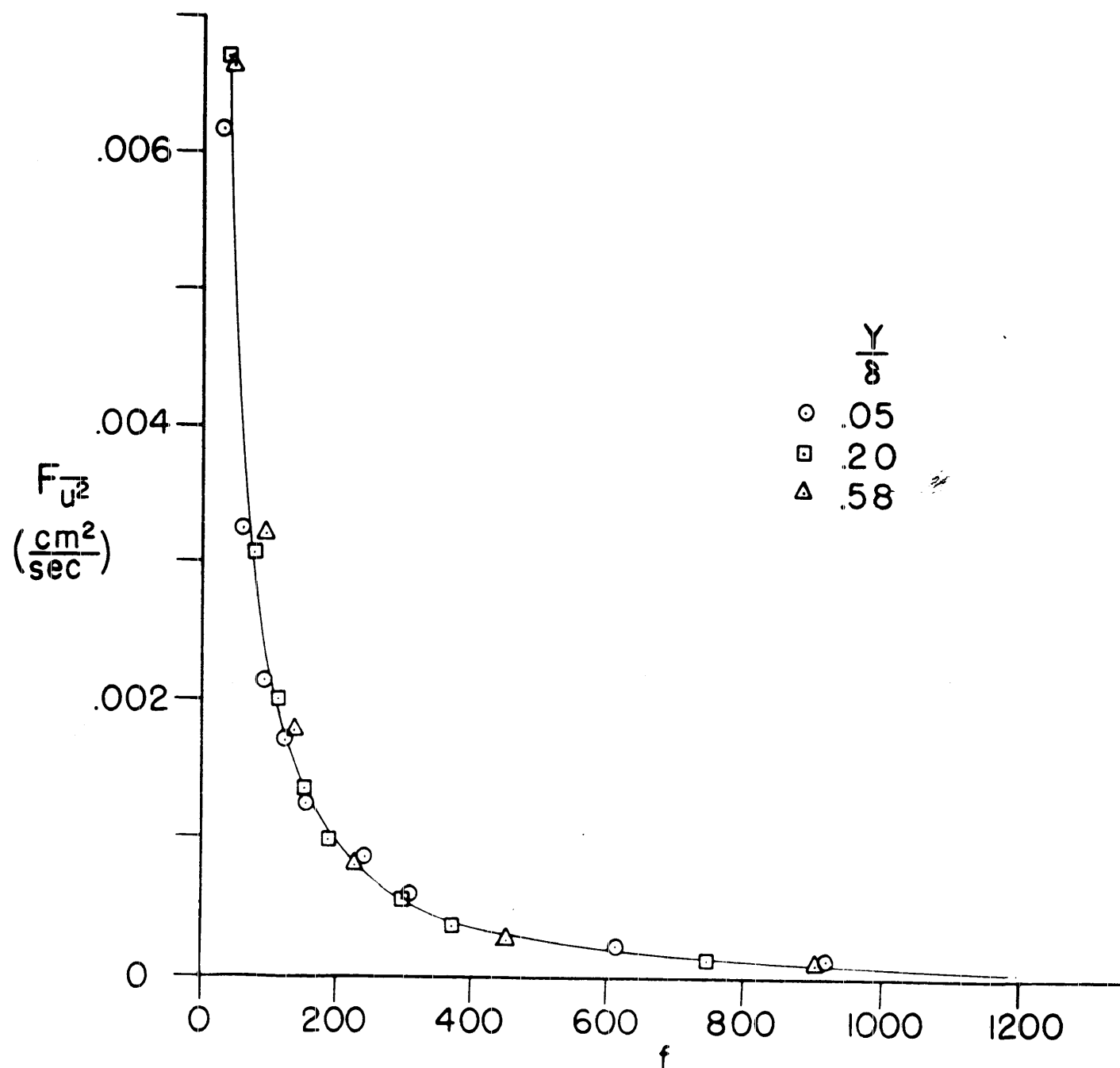


Figure 5. Normalized Energy Spectra at $y/\delta = .05$ Across Boundary Layer.

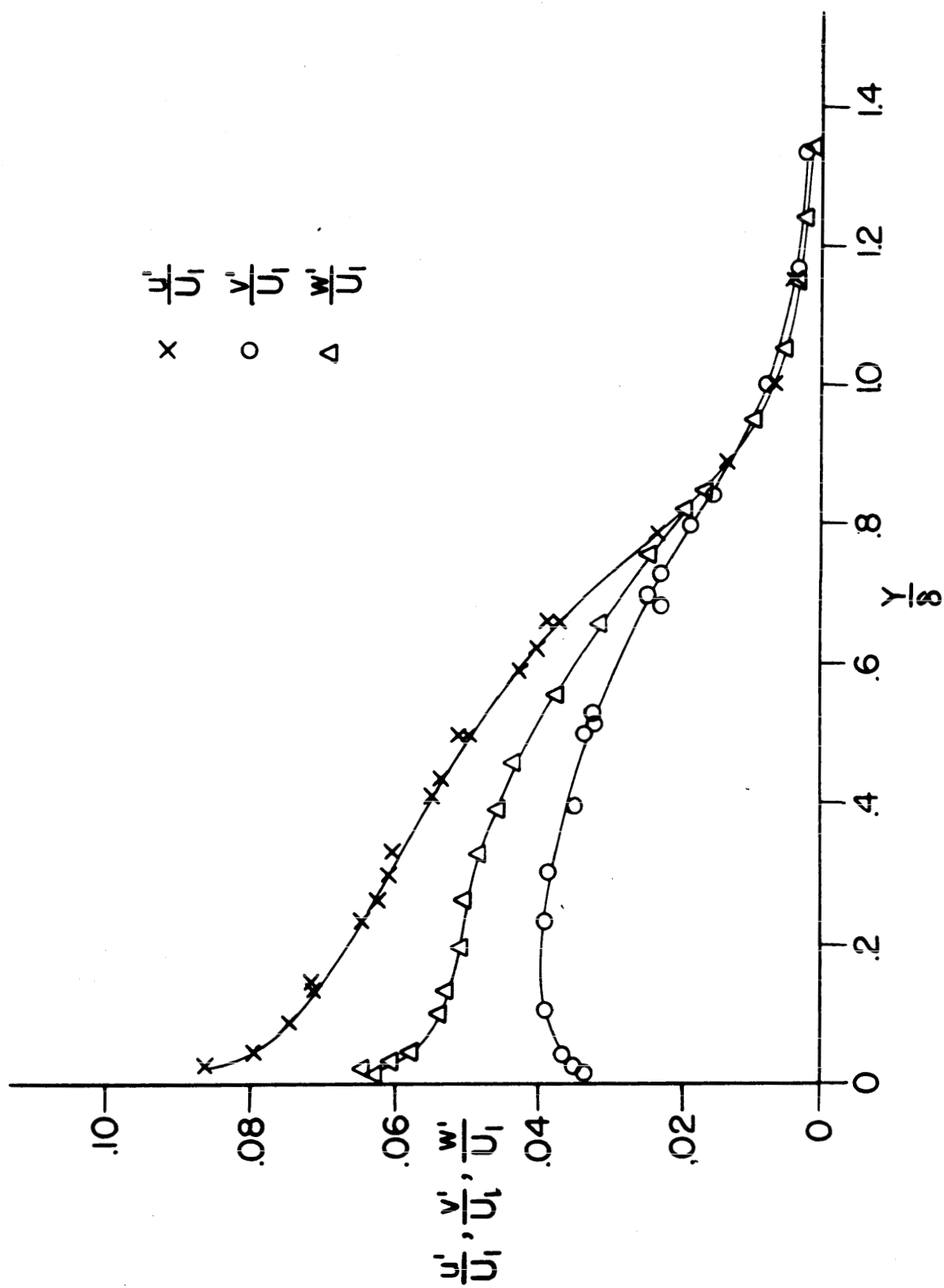


Figure 6. Variation of Fluctuation Levels Across Boundary Layer.

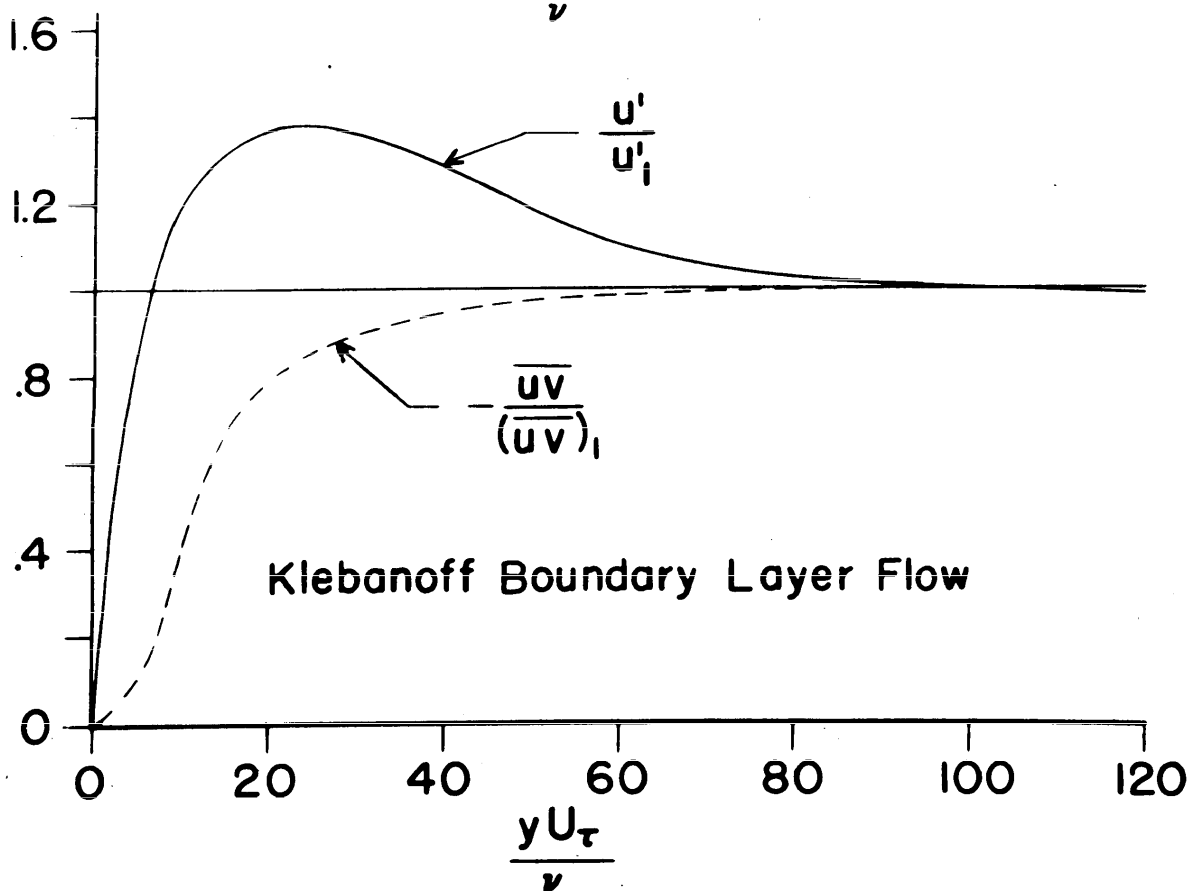
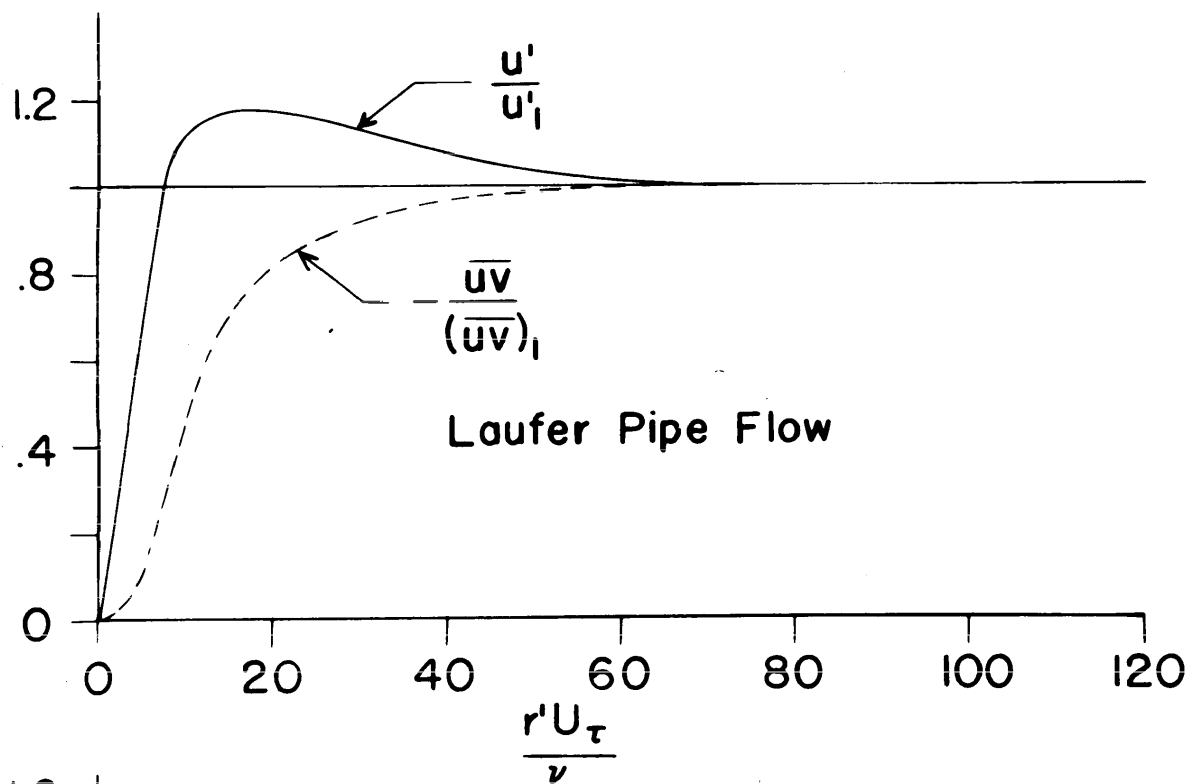


Figure 7. Fluctuation Level and Turbulent Shear Stress Near the Wall
~~from~~ Klebanoff and Laufer.

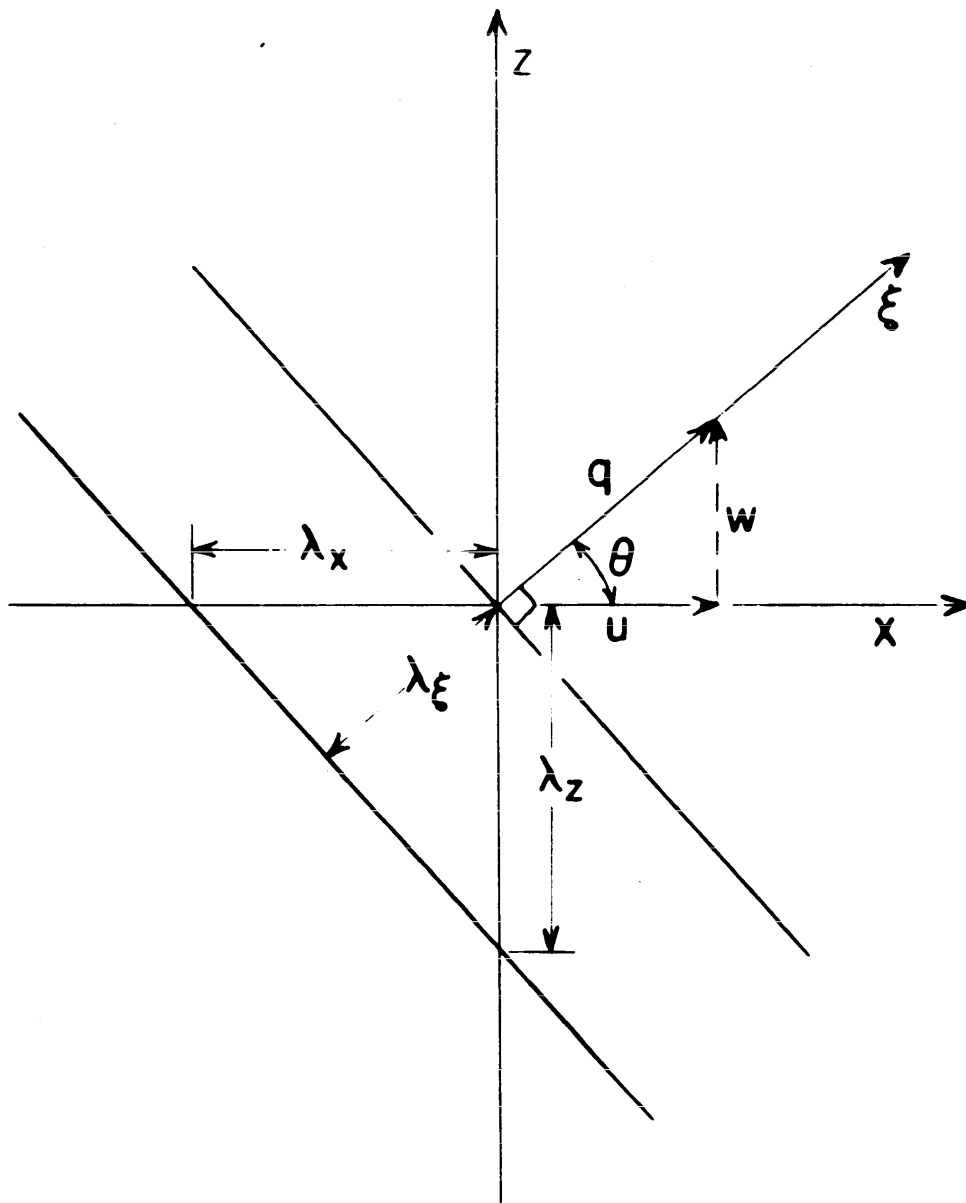


Figure 8. Assumed Form of Oblique Disturbance at Edge of Sublayer.

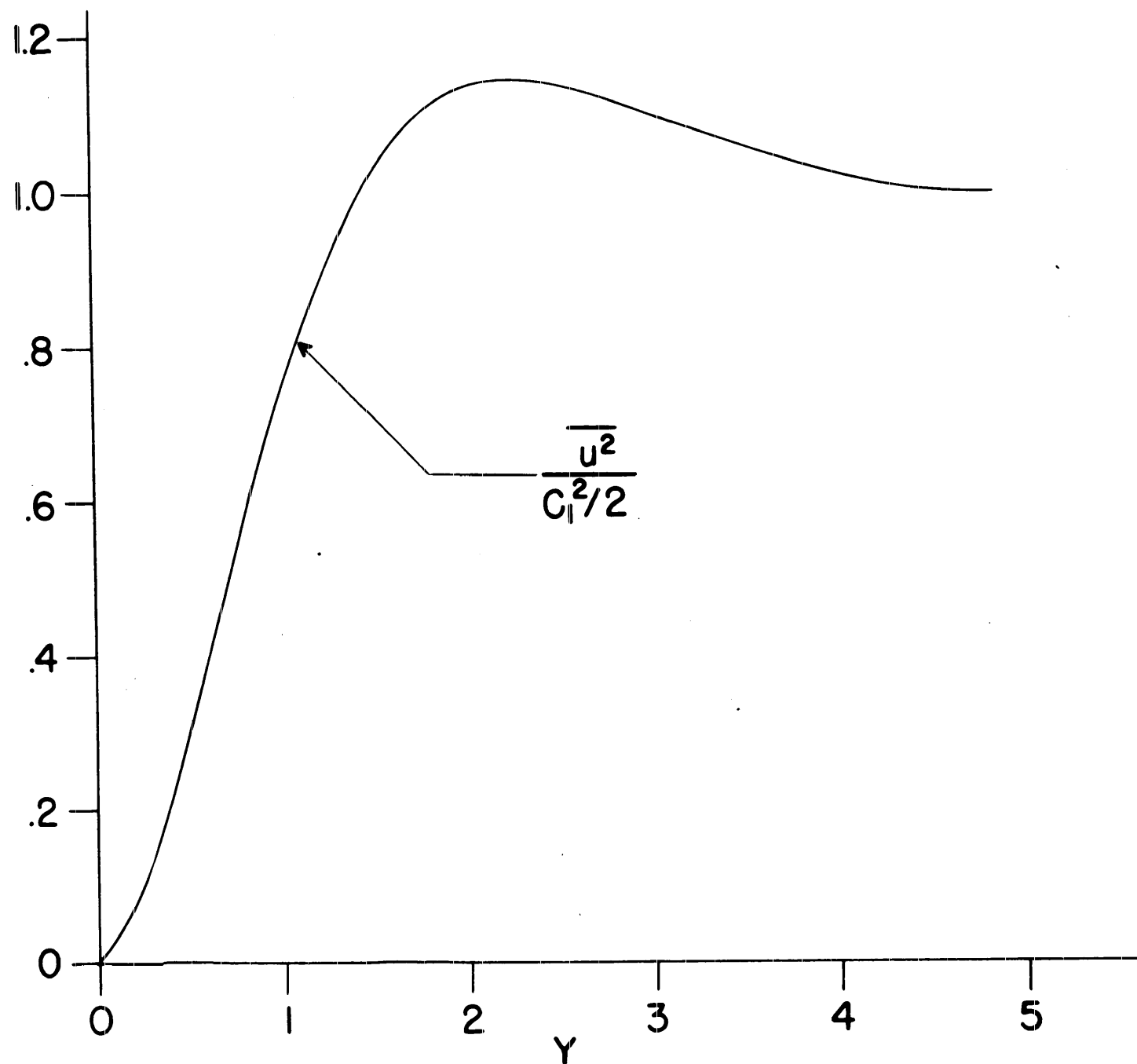


Figure 9. Theoretical Variation of Fluctuation Energy in the Viscous Region.

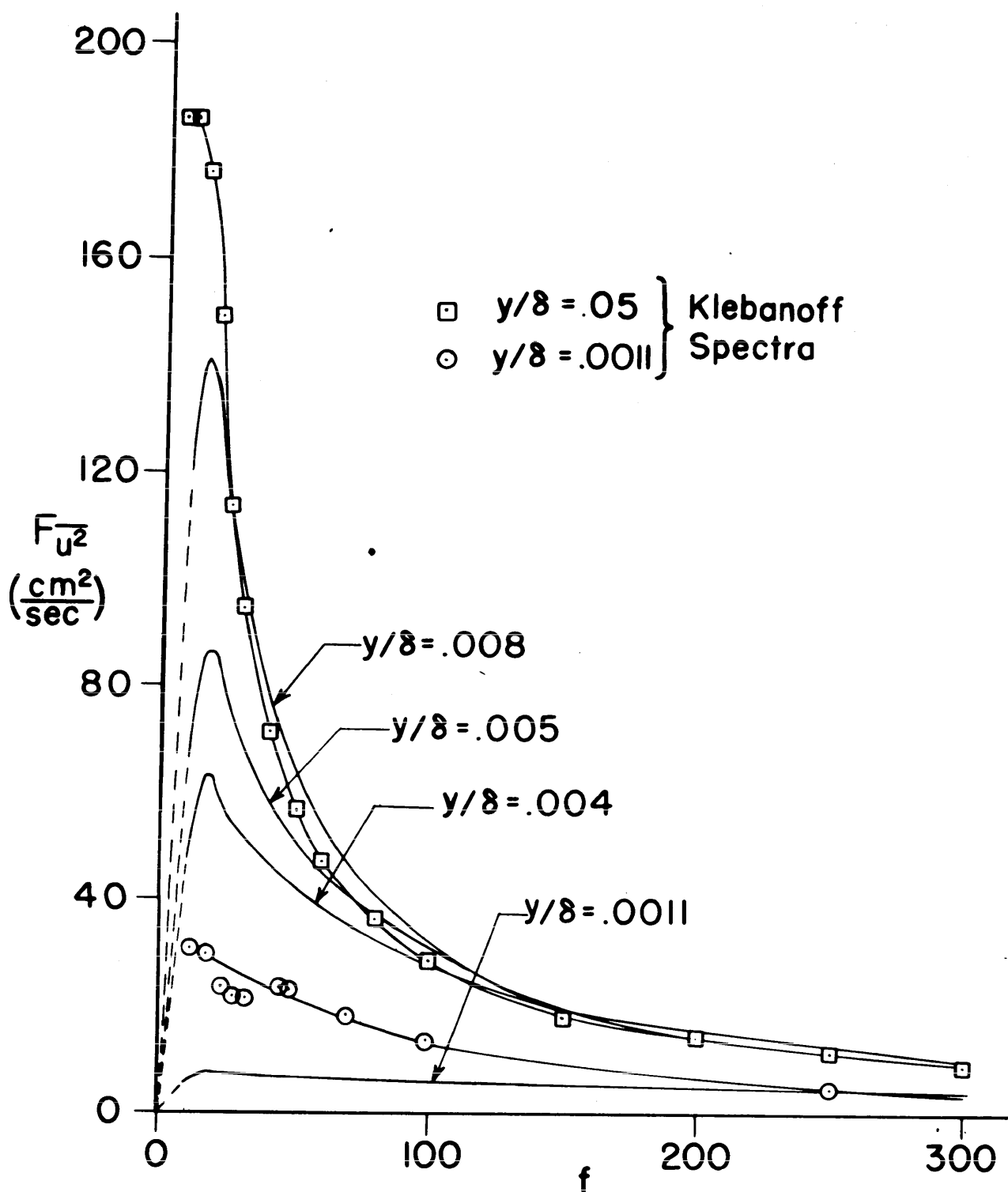


Figure 10. Energy Spectra in the Sublayer Based on Spectrum Outside Sublayer.

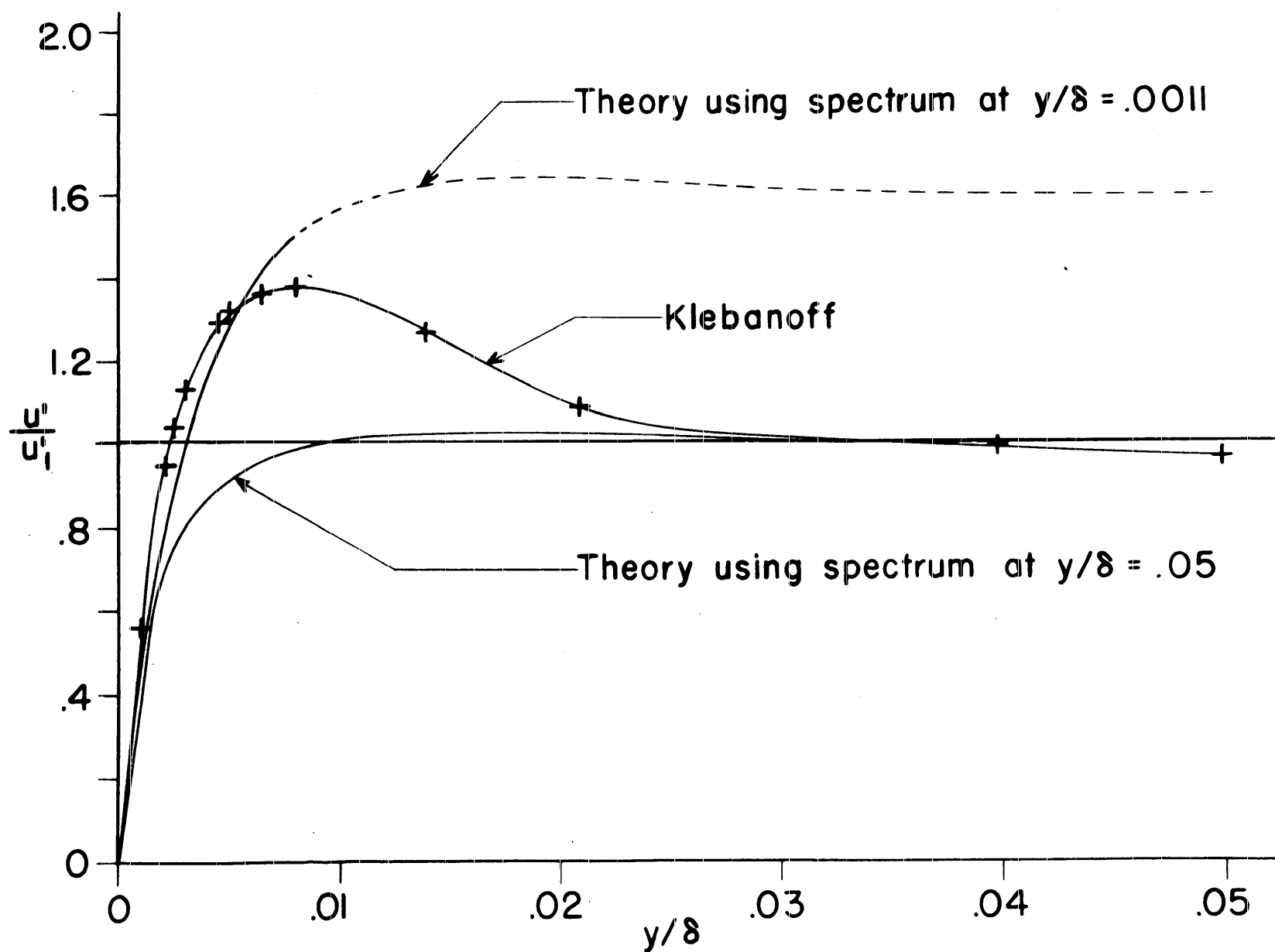


Figure 11. (a) Comparison of Theory and Experiment for Turbulent Fluctuations in the Sublayer - Boundary Layer.

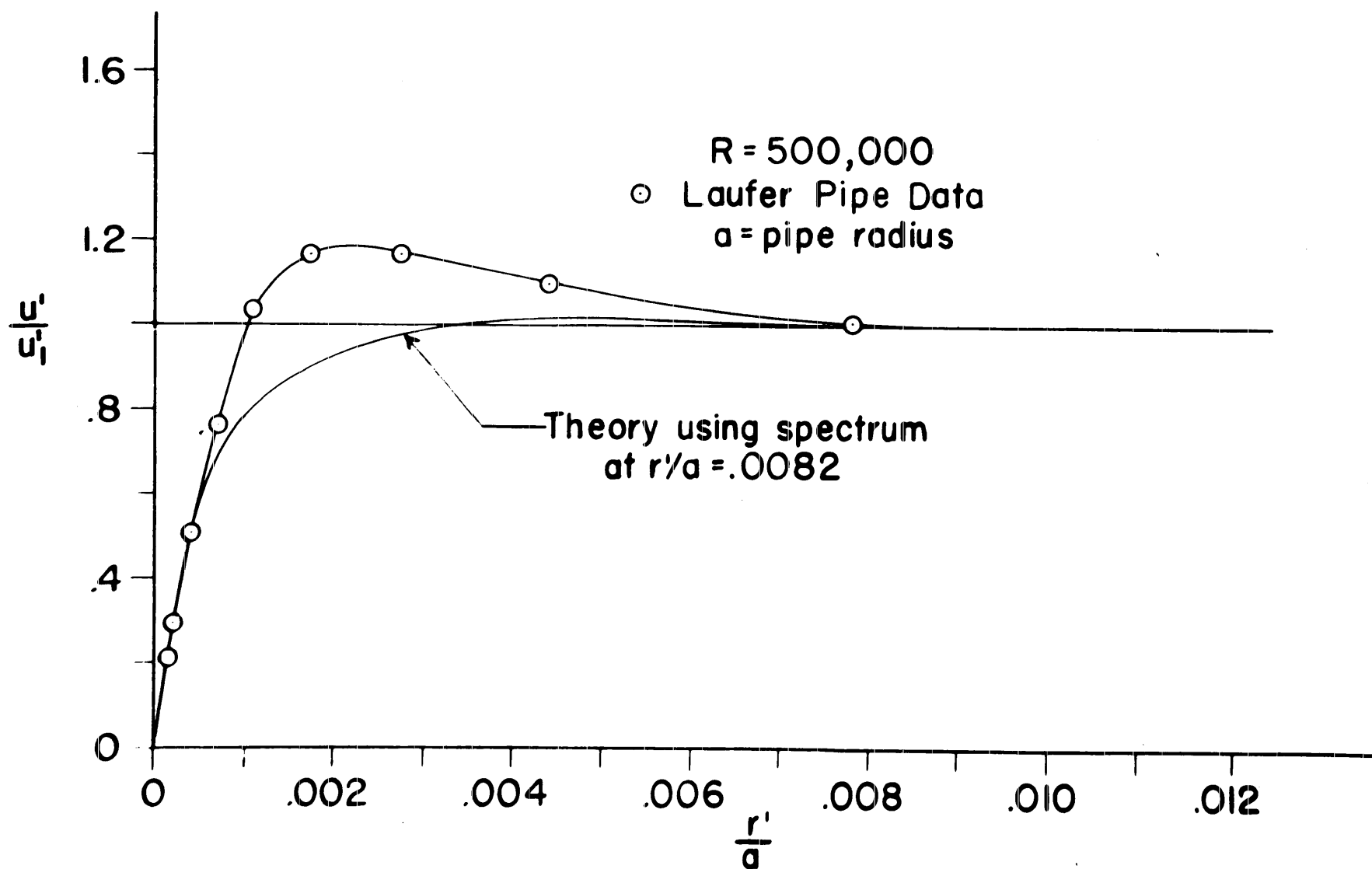


Figure 11. (b) Comparison of Theory and Experiment for Turbulent Fluctuations in the Sublayer - Pipe Flow.

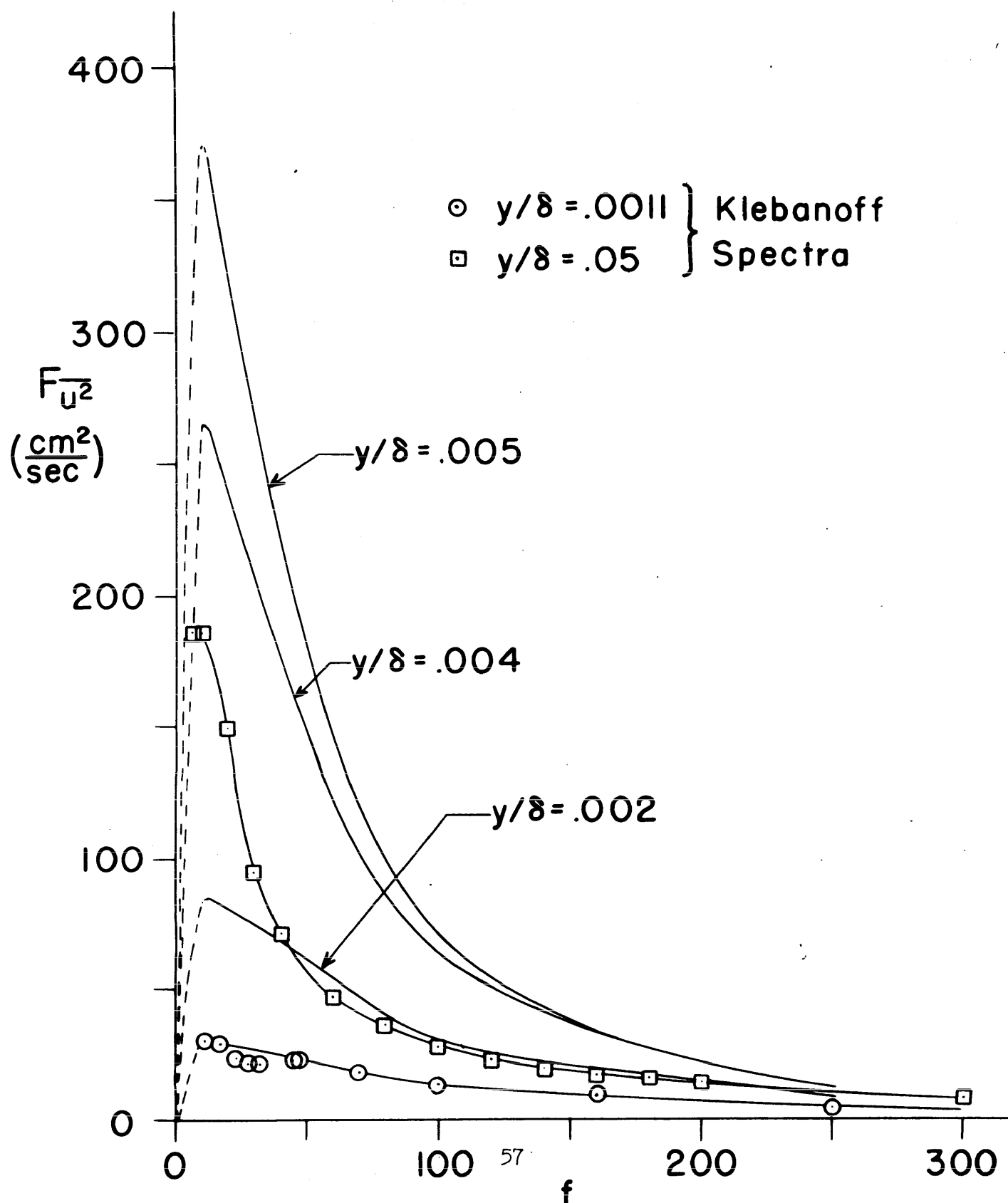


Figure 12. Energy Spectra in the Sublayer Based on Spectrum Inside Sublayer.

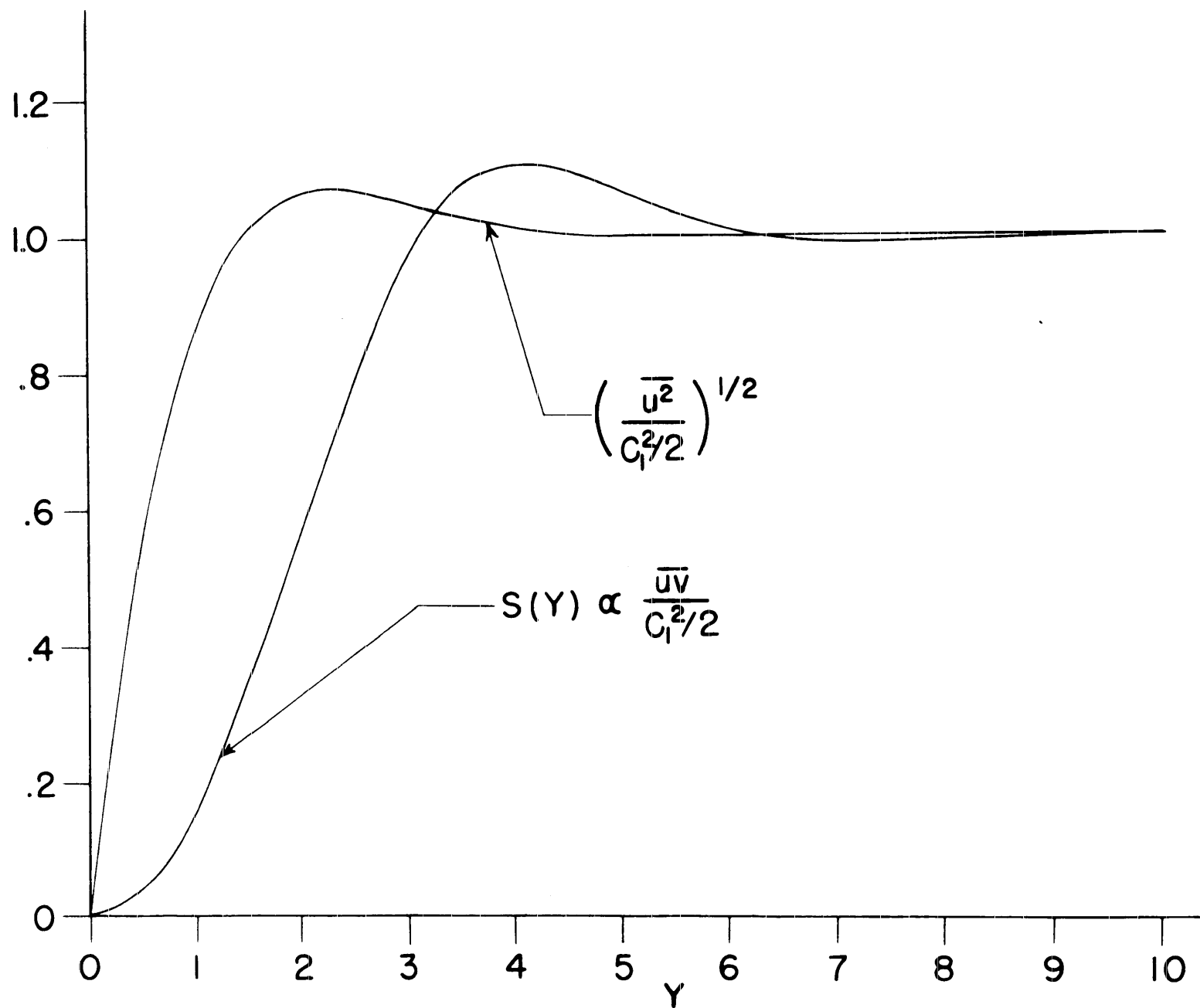


Figure 13. Theoretical Variation of Fluctuation Level and Turbulent Shear Stress in the Viscous Region.

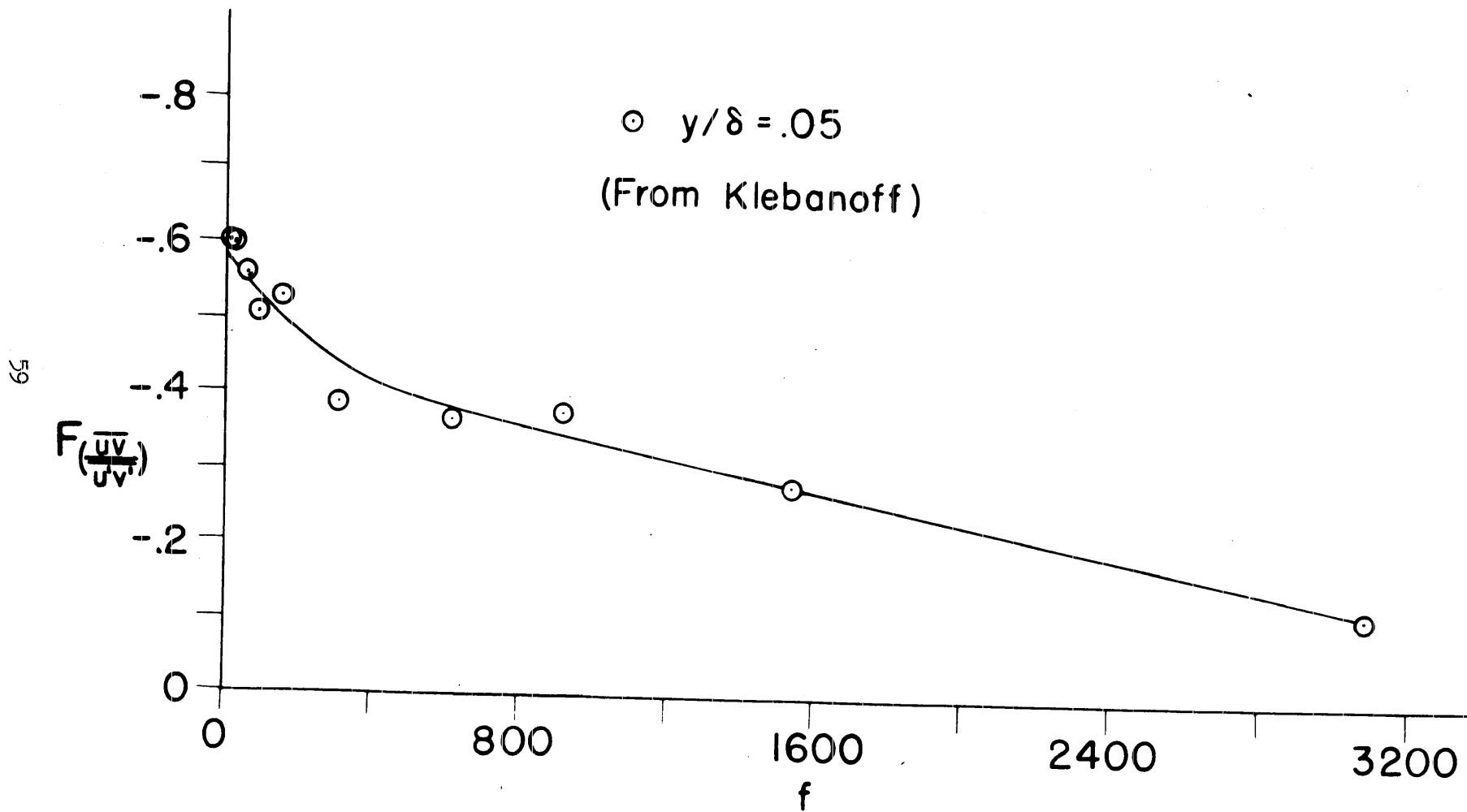


Figure 14. Variation of Shear Correlation Coefficient with Frequency Outside Sublayer after Klebanoff.

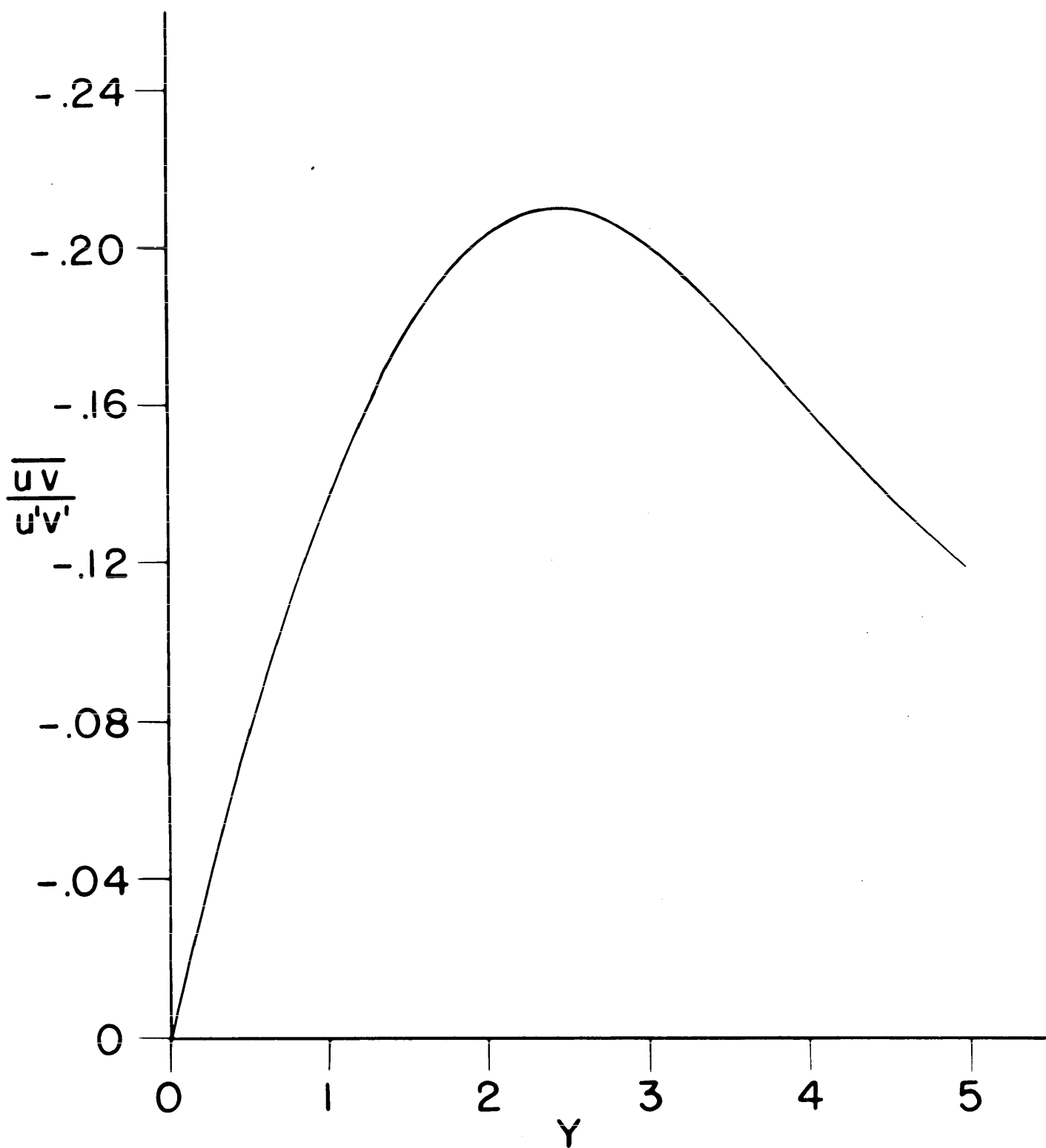


Figure 15. Theoretical Variation of Shear Correlation Coefficient in the Viscous Region.

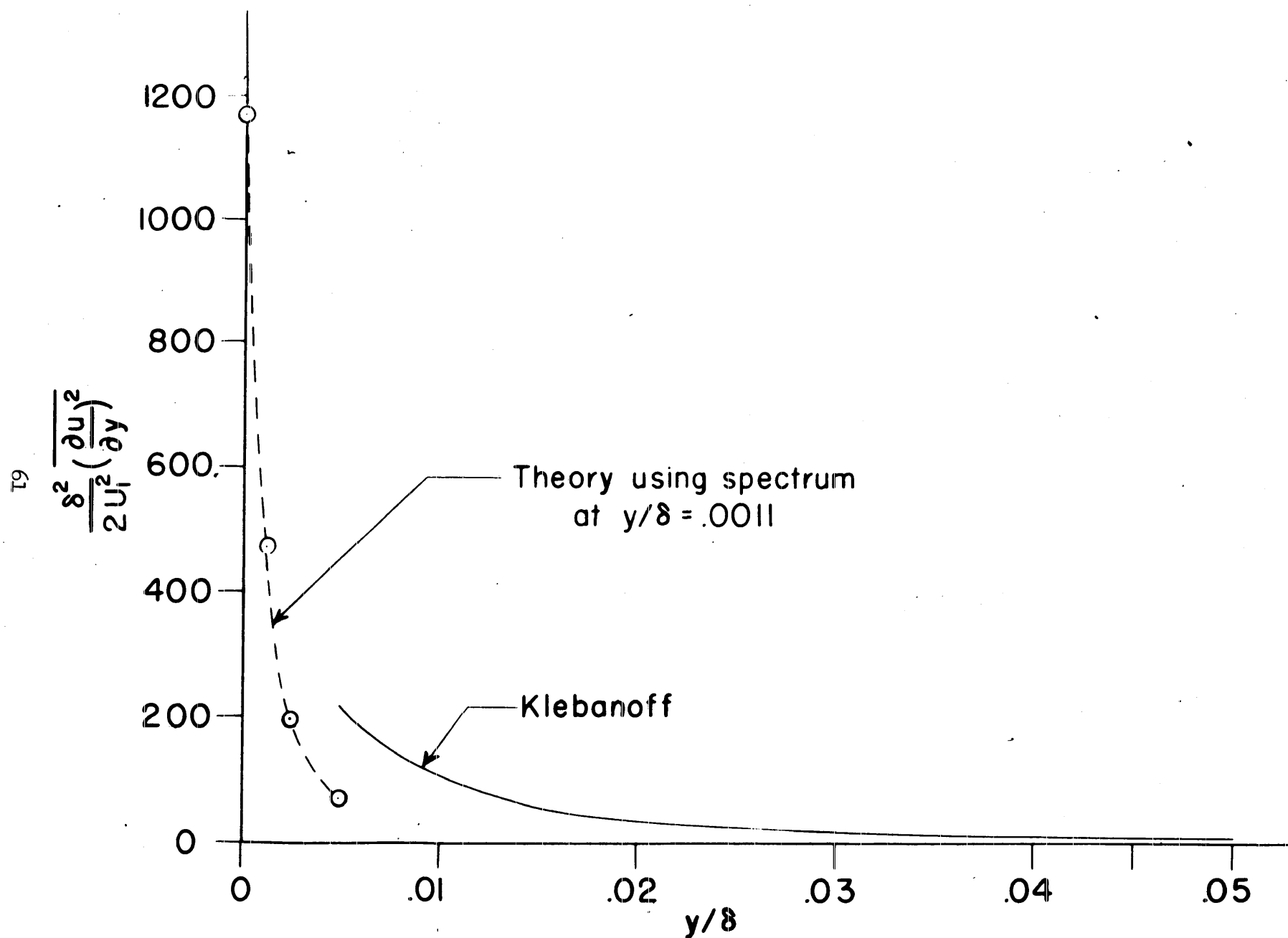


Figure 16. Comparison of Theory and Experiment for Transverse Microscale in the Sublayer.

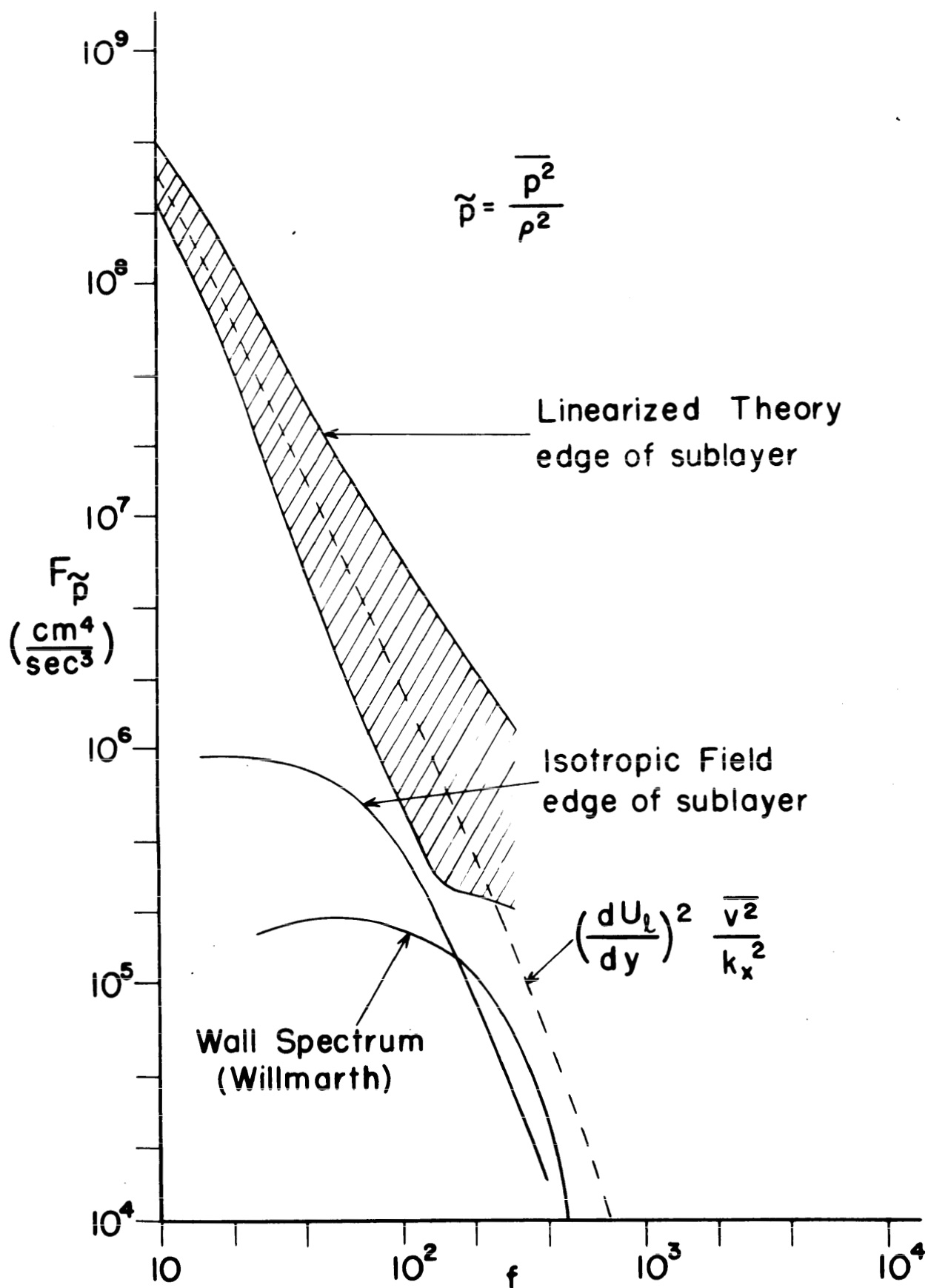
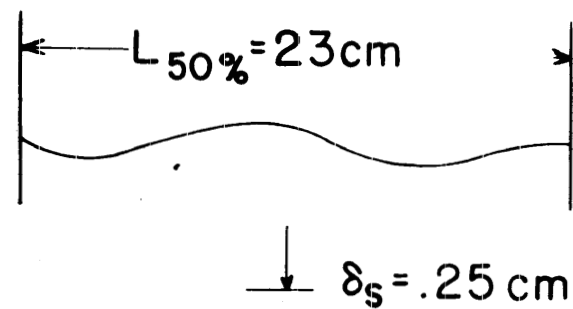


Figure 17. Pressure Fluctuation Spectra at Edge of Sublayer and at Wall.

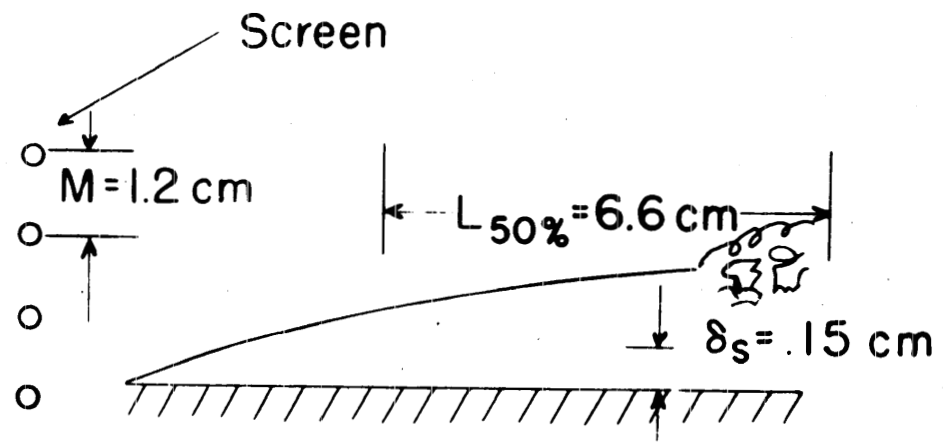


$$U_1 = 1.52 \times 10^3 \text{ cm/sec}$$

$$\delta = 7.6 \text{ cm}$$

$$R_\delta = 7.9 \times 10^4$$

Turbulent boundary layer



$$U_1 = 9.9 \times 10^2 \text{ cm/sec}$$

$$\delta_{tr} = .28 \text{ cm} \quad \frac{u'}{U_1} = .03$$

$$Re_{tr} = 1 \times 10^5$$

Laminar-Turbulent transition

Figure 18. Comparison of Sublayers for Boundary Layer Turbulence and Free Stream Turbulence.

Page intentionally blank

Page intentionally blank

Page intentionally blank

DISTRIBUTION LIST

<u>No. of Copies</u>	<u>Organization</u>	<u>No. of Copies</u>	<u>Organization</u>
1	Chief of Ordnance ATTN: ORDTB - Bal Sec Department of the Army Washington 25, D. C.	1	Commander Naval Ordnance Test Station ATTN: Dr. H. R. Kelly China Lake, California
1	Commanding Officer Diamond Ordnance Fuze Laboratories ATTN: Technical Information Office, Branch 012 Washington 25, D. C.	1	Commanding Officer and Director U. S. Navy Underwater Sound Laboratory ATTN: Mr. W. A. Von Winkle Fort Trumbull New London, Connecticut
10	Commander Armed Services Technical Information Agency ATTN: TIPCR Arlington Hall Station Arlington 12, Virginia	1	Director National Aeronautics and Space Administration ATTN: Mr. C. E. Brown Langley Research Center Langley Field, Virginia
10	Commander British Army Staff British Defence Staff (W) ATTN: Reports Officer 3100 Massachusetts Avenue, N.W. Washington 8, D. C.	2	Director National Aeronautics and Space Administration ATTN: Mr. H. J. Allen Dr. A. Eggers Ames Research Center Moffett Field, California
4	Defence Research Member Canadian Joint Staff 2450 Massachusetts Avenue, N.W. Washington 8, D. C.	1	Director National Aeronautics and Space Administration ATTN: Dr. H. L. Dryden, Deputy Administrator 1520 H. Street, N.W. Washington 25, D. C.
3	Chief, Bureau of Naval Weapons ATTN: DIS-33 Department of the Navy Washington 25, D. C.		
2	Commander U. S. Naval Weapons Laboratory Dahlgren, Virginia	1	Army Research Office Arlington Hall Station Arlington 6, Virginia
2	Commander Naval Ordnance Laboratory ATTN: Dr. R. Wilson Dr. K. Lobb White Oak Silver Spring 19, Maryland	1	AVCO Manufacturing Corporation Research and Advanced Development Division 201 Lowell Street Wilmington, Massachusetts

DISTRIBUTION LIST

<u>No. of Copies</u>	<u>Organization</u>	<u>No. of Copies</u>	<u>Organization</u>
1	Gas Dynamics Facility ARO, Inc. ATTN: Mr. J. Lukasiewicz Tullahoma, Tennessee	1	Catholic University of America ATTN: Professor M. Monk Department of Physics Washington 17, D. C.
1	Lockheed Missile Systems Division ATTN: Mr. R. Smelt Box 504 Sunnyvale, California	1	Harvard University Department of Applied Physics and Engineering Science ATTN: Dr. A. Bryson Cambridge 38, Massachusetts
3	The Martin Company ATTN: Dr. M. Morkovin, Chief, Aerophysics Research Flight, Vehicle Design Department Dr. S. Traugott Baltimore 3, Maryland	2	The Johns Hopkins University Department of Aeronautics ATTN: Dr. L. Kovasznay Dr. F. H. Clauser Baltimore 18, Maryland
1	North American Aviation, Inc. Aeronautical Laboratory ATTN: Dr. E. R. Van Driest Downey, California	1	The Johns Hopkins University Mechanical Engineering Department ATTN: Professor S. Corrsin Baltimore, Maryland
2	Guggenheim Aeronautical Laboratory California Institute of Technology ATTN: Dr. C. B. Millikan Professor H. W. Liepmann Pasadena 4, California	1	New York University Department of Aeronautics ATTN: Dr. J. F. Ludlow University Heights New York 53, New York
1	Jet Propulsion Laboratory 4800 Oak Grove Drive ATTN: Dr. John Laufer Pasadena, California	1	Ohio State University Aeronautical Engineering Department ATTN: Professor G. L. von Eschen Columbus, Ohio
1	Brown University ATTN: J. Kestin, Professor of Engineering Providence 12, Rhode Island	1	Pennsylvania State College Department of Aeronautical Engineering ATTN: Professor M. Lessen State College, Pennsylvania
1	Cornell University Graduate School of Aeronautical Engineering ATTN: Dr. W. R. Sears Ithaca, New York	1	The Pennsylvania State University Ordnance Research Laboratory ATTN: John L. Lumley, Assistant Professor of Engineering Research University Park, Pennsylvania

DISTRIBUTION LIST

<u>No. of Copies</u>	<u>Organization</u>	<u>No. of Copies</u>	<u>Organization</u>
1	Polytechnic Institute of Brooklyn Aerodynamics Laboratory ATTN: Dr. A. Ferri 527 Atlantic Avenue Freeport, New York	1	University of Illinois Chemical Engineering Department ATTN: Professor T. J. Hanratty Urbana, Illinois
1	Purdue University School of Aeronautical Engineering ATTN: Professor Harold De Groff Lafayette, Indiana	3	University of Michigan Department of Aeronautical Engineering ATTN: Dr. Arnold Kuethe Dr. Mahinder Uberoi Professor Wilbur Nelson East Engineering Building Ann Arbor, Michigan
2	Princeton University Forrestal Research Center Aeronautics Department ATTN: Professor S. Bogdonoff Professor W. Hayes Princeton, New Jersey	1	University of Minnesota Department of Mechanical Engineering ATTN: Dr. E. R. G. Eckert Division of Thermodynamics Minneapolis 14, Minnesota
1	Rensselaer Polytechnic Institute Aerodynamics Department ATTN: Dr. J. V. Foa Troy, New York	1	University of Washington Department of Aeronautical Engineering ATTN: Professor R. E. Street Seattle 5, Washington
1	Southwest Research Institute Department of Applied Mechanics ATTN: Mr. W. Squire 8500 Culebra Road San Antonio, Texas	1	Professor H. W. Emmons Harvard University Cambridge 38, Massachusetts
2	Stanford University ATTN: W. G. Vincenti, Aerodynamics Department Miss Phyllis Flanders, Department of Physics Menlo Park, California	1	Dr. A. E. Puckett Systems Development Laboratories Hughes Aircraft Company Culver City, California
1	University of California ATTN: Professor G. M. Corcos College of Engineering Berkeley 4, California	1	Dr. Theodore von Karman Chairman, AGARD APO 230, New York, New York
2	University of Illinois Department of Aeronautical Engineering ATTN: Professor H. S. Stillwell Dr. Bruce Hicks Urbana, Illinois		

AD Accession No.
Ballistic Research Laboratories, APG
A THEORY FOR THE LAMINAR SUBLAYER OF A TURBULENT FLOW
Joseph Sternberg
BRL Report No. 1127 April 1961
DA Proj No. 503-03-009, OMSC No. 5210.11.140
UNCLASSIFIED Report

UNCLASSIFIED
Fluid flow - Turbulence
Laminar boundary layer -
Mathematical analysis
Aerodynamics - Theory

The so-called laminar sublayer is shown to be the region where the turbulent velocity fluctuations are directly dissipated by viscosity. A simplified linearized form of the equations of motion for the turbulent fluctuations is used to describe the turbulent field between the wall and the fully turbulent part of the flow. The mean flow in the sublayer and the turbulence field outside the sublayer are assumed to be known from the experiments. The thickness of the sublayer arises naturally in the theory. It is shown that the large scale fluctuations containing most of the turbulent energy are convected downstream with a velocity characteristic of the middle of the boundary layer. Thus Taylor's hypothesis does not apply to these large scale fluctuations near the wall. Calculations are given for the energy spectra and u' fluctuation level in the sublayer and other aspects of the fluctuation field are discussed. Examining the effect of strong free stream turbulence on laminar boundary layer transition, it appears that the physical model underlying Taylor's parameter is incorrect.

AD Accession No.
Ballistic Research Laboratories, APG
A THEORY FOR THE LAMINAR SUBLAYER OF A TURBULENT FLOW
Joseph Sternberg
BRL Report No. 1127 April 1961
DA Proj No. 503-03-009, OMSC No. 5210.11.140
UNCLASSIFIED Report

UNCLASSIFIED
Fluid flow - Turbulence
Laminar boundary layer -
Mathematical analysis
Aerodynamics - Theory

The so-called laminar sublayer is shown to be the region where the turbulent velocity fluctuations are directly dissipated by viscosity. A simplified linearized form of the equations of motion for the turbulent fluctuations is used to describe the turbulent field between the wall and the fully turbulent part of the flow. The mean flow in the sublayer and the turbulence field outside the sublayer are assumed to be known from the experiments. The thickness of the sublayer arises naturally in the theory. It is shown that the large scale fluctuations containing most of the turbulent energy are convected downstream with a velocity characteristic of the middle of the boundary layer. Thus Taylor's hypothesis does not apply to these large scale fluctuations near the wall. Calculations are given for the energy spectra and u' fluctuation level in the sublayer and other aspects of the fluctuation field are discussed. Examining the effect of strong free stream turbulence on laminar boundary layer transition, it appears that the physical model underlying Taylor's parameter is incorrect.

AD Accession No.
Ballistic Research Laboratories, APG
A THEORY FOR THE LAMINAR SUBLAYER OF A TURBULENT FLOW
Joseph Sternberg
BRL Report No. 1127 April 1961
DA Proj No. 503-03-009, OMSC No. 5210.11.140
UNCLASSIFIED Report

UNCLASSIFIED
Fluid flow - Turbulence
Laminar boundary layer -
Mathematical analysis
Aerodynamics - Theory

The so-called laminar sublayer is shown to be the region where the turbulent velocity fluctuations are directly dissipated by viscosity. A simplified linearized form of the equations of motion for the turbulent fluctuations is used to describe the turbulent field between the wall and the fully turbulent part of the flow. The mean flow in the sublayer and the turbulence field outside the sublayer are assumed to be known from the experiments. The thickness of the sublayer arises naturally in the theory. It is shown that the large scale fluctuations containing most of the turbulent energy are convected downstream with a velocity characteristic of the middle of the boundary layer. Thus Taylor's hypothesis does not apply to these large scale fluctuations near the wall. Calculations are given for the energy spectra and u' fluctuation level in the sublayer and other aspects of the fluctuation field are discussed. Examining the effect of strong free stream turbulence on laminar boundary layer transition, it appears that the physical model underlying Taylor's parameter is incorrect.

AD Accession No.
Ballistic Research Laboratories, APG
A THEORY FOR THE LAMINAR SUBLAYER OF A TURBULENT FLOW
Joseph Sternberg
BRL Report No. 1127 April 1961
DA Proj No. 503-03-009, OMSC No. 5210.11.140
UNCLASSIFIED Report

UNCLASSIFIED
Fluid flow - Turbulence
Laminar boundary layer -
Mathematical analysis
Aerodynamics - Theory

The so-called laminar sublayer is shown to be the region where the turbulent velocity fluctuations are directly dissipated by viscosity. A simplified linearized form of the equations of motion for the turbulent fluctuations is used to describe the turbulent field between the wall and the fully turbulent part of the flow. The mean flow in the sublayer and the turbulence field outside the sublayer are assumed to be known from the experiments. The thickness of the sublayer arises naturally in the theory. It is shown that the large scale fluctuations containing most of the turbulent energy are convected downstream with a velocity characteristic of the middle of the boundary layer. Thus Taylor's hypothesis does not apply to these large scale fluctuations near the wall. Calculations are given for the energy spectra and u' fluctuation level in the sublayer and other aspects of the fluctuation field are discussed. Examining the effect of strong free stream turbulence on laminar boundary layer transition, it appears that the physical model underlying Taylor's parameter is incorrect.